



HAL
open science

Cardenolides, toxicity, and the costs of sequestration in the coevolutionary interaction between monarchs and milkweeds

Anurag A Agrawal, Katalin Böröczky, Meena Haribal, Amy P Hastings, Ron A White, Ren-Wang Jiang, Christophe Duplais

► **To cite this version:**

Anurag A Agrawal, Katalin Böröczky, Meena Haribal, Amy P Hastings, Ron A White, et al.. Cardenolides, toxicity, and the costs of sequestration in the coevolutionary interaction between monarchs and milkweeds. *Proceedings of the National Academy of Sciences of the United States of America*, 2021, 118 (16), pp.e2024463118. 10.1073/pnas.2024463118 . hal-03217023

HAL Id: hal-03217023

<https://hal.science/hal-03217023>

Submitted on 5 May 2021

HAL is a multi-disciplinary open access archive for the deposit and dissemination of scientific research documents, whether they are published or not. The documents may come from teaching and research institutions in France or abroad, or from public or private research centers.

L'archive ouverte pluridisciplinaire **HAL**, est destinée au dépôt et à la diffusion de documents scientifiques de niveau recherche, publiés ou non, émanant des établissements d'enseignement et de recherche français ou étrangers, des laboratoires publics ou privés.

Main Manuscript for

Cardenolides, toxicity and the costs of sequestration in the coevolutionary interaction between monarchs and milkweeds

Anurag A. Agrawal^{1, 2*}
Katalin Böröczky¹
Meena Haribal³
Amy P. Hastings¹
Ron A. White¹
Ren-Wang Jiang⁴
Christophe Duplais⁵

¹ Department of Ecology and Evolutionary Biology, Cornell University, Ithaca, NY (USA)

² Department of Entomology, Cornell University, Ithaca, NY (USA)

³ 1406 Slaterville Road, Ithaca, NY (USA)

⁴ Guangdong Province Key Laboratory of Pharmacodynamic Constituents of Traditional Chinese Medicine and New Drugs Research, College of Pharmacy, Jinan University, Guangzhou 510632 (China)

⁵ CNRS, UMR8172 EcoFoG, AgroParisTech, Cirad, INRAE, Université des Antilles, Université de Guyane, Campus agronomique, avenue de France, 97379 Kourou, French Guiana (France)

*correspondence: agrawal@cornell.edu

Classification

Major: Evolution (Biological Science)

Minor: Ecology (Biological Science)

Keywords:

Chemical ecology, coevolution, monarch butterfly (*Danaus plexippus*), milkweeds *Asclepias*, plant defense theory, plant-insect interactions, toxin sequestration

Abstract

For highly specialized insect herbivores, plant chemical defenses are often coopted as cues for oviposition and sequestration. In such interactions, can plants evolve novel defenses, pushing herbivores to trade off benefits of specialization with costs of coping with toxins? We tested how variation in milkweed toxins (cardenolides) impacted monarch butterfly (*Danaus plexippus*) growth, sequestration, and oviposition when consuming tropical milkweed (*Asclepias curassavica*), one of two critical host plants worldwide. The most abundant leaf toxin, highly apolar and thiazolidine ring-containing voruscharin, accounted for 40% of leaf cardenolides, negatively predicted caterpillar growth, and was not sequestered. Using whole plants and purified voruscharin, we show that monarch caterpillars convert voruscharin to calotropin and calactin *in vivo*, imposing a burden on growth. As shown by *in vitro* experiments, this conversion is facilitated by temperature and alkaline pH. We next employed toxin-target site experiments with isolated cardenolides and the monarch's neural Na⁺/K⁺-ATPase, revealing that voruscharin is highly inhibitory compared to several standards and sequestered cardenolides. The monarch's typical >50-fold enhanced resistance to cardenolides compared to sensitive animals was absent for voruscharin, suggesting highly specific plant defense. Finally, oviposition was greatest on intermediate cardenolide plants, supporting the notion of a trade-off between benefits and costs of sequestration for this highly specialized herbivore. There is apparently ample opportunity for continued coevolution between monarchs and milkweeds, although the diffuse nature of the interaction, due to migration and interaction with multiple milkweeds, may limit the ability of monarchs to counter-adapt.

Significant statement

Interactions between plants and herbivores constitute a major pathway of energy transfer up the food chain. As a consequence, evolution by natural selection has honed the chemically-mediated antagonistic interactions between these groups of organisms. Monarch butterflies and milkweeds serve as royal representatives in deciphering such coevolution, and our study takes a mechanistic and manipulative approach to understand how the tropical milkweed, *Asclepias curassavica*, defends itself against monarch butterflies, which would seem to be impervious feeders. By directly observing plant-herbivore interactions and coupling this with

experiments on isolated toxins and the monarch's neural sodium-potassium pump enzymes, we show that tropical milkweed produces a burdensome cardenolide toxin and monarchs convert it to less toxic compounds, the latter sequestered for their own benefit.

Introduction

Although coevolutionary interactions are often portrayed as simplified arms races of reciprocal defense and offense evolution, the dynamics are decidedly more complex. For example, how do plants respond to highly specialized herbivores, and are such adapted consumers immune to plant defenses? On average, specialists are less impacted by particular plant defense compounds than generalists (1, 2), but does this mean that further coevolution is not possible? Even highly specialized herbivores must contend with plant defenses if coevolutionary interactions are proceeding (3). For any herbivorous insect, larval feeding, protection from enemies, and adult oviposition are each key points in the life-cycle where plant chemistry plays a role in the outcome. Thus, the typical cornucopia of chemical compounds in an individual plant presents opportunities for both plant resistance and cooption of this defense by specialist herbivores (4-6).

It is thus far unclear how often coevolutionary interactions reach equilibrium or "stalemate" as it were (7). Nonetheless, several conditions are predicted to slow or suppress the endless arms race. First, the more specialized an interaction, the greater the investments required and potential challenges to innovation. Second, when different life-stages of herbivores are subject to distinct selection pressures (8-10), continued coevolution may be restricted because of conflicting selection. And finally, when aspects of the population biology of the species involved reduce local adaptation, such as gene flow and the presence of alternate hosts, asymmetry may emerge in the coevolutionary match between plants and herbivores (11, 12). In the interaction between milkweed plants and monarch butterflies, cardenolides have played a central role in our understanding of coevolutionary specialization, larval feeding, sequestration, and to a lesser extent, oviposition (13). Although monarchs are abundant across a broad geographical range, substantial phenotypic and genetic analyses have failed to reveal population differentiation (14, 15). A lack of local adaptation is likely due to the four-generation annual cycle, where butterflies feed on diverse milkweed species and yet intermix during migration and overwintering (13).

There is some evidence that cardenolides can be a burden for monarch caterpillars (16-20), although costs of sequestration have not been demonstrated. Nonetheless, many assays, even across >10-fold concentrations of cardenolides, fail to show negative effects of cardenolides on monarchs (21). More mechanistic *in vitro* work with the monarch's highly resistant sodium-potassium pump (Na^+/K^+ -ATPase), the cellular target of cardenolides, demonstrated that some milkweed cardenolides are strong inhibitors of monarch neural physiology (22). Thus, work with specific compounds that are variable in plants is needed to pinpoint agents of resistance. For sequestration of cardenolides, a model proposed by Nelson (23) and supported in a review of early work (24) and new research (25) suggests that monarchs selectively sequester more polar cardenolides, some compounds are metabolized

(modification or detoxification), and others are transported via carriers (20, 26-28). Finally, observational work indicated that monarchs tend to oviposit on intermediate cardenolide concentration plants (29, 30), suggesting the hypothesis that adult butterflies minimize toxic exposure to larvae while optimizing sequestration of plant poisons.

Asclepias curassavica is surprisingly understudied in its interactions with monarch butterflies, despite being a critical hostplant worldwide (second only to *A. syriaca*) (13). Attack of *A. curassavica* by monarchs can be strong, and therefore a likely source of selection for plant defense. The species is weedy throughout the tropics and has a plethora of cardenolides, including relatively uncommon compounds, some of which may be detrimental to monarch performance (20, 28, 31-34). In particular, voruscharin is a long-known cardenolide containing a thiazolidine heterocycle (having both nitrogen and sulfur, Fig. 1), yet its previous study was hampered by solubility issues and the inability of thin layer chromatography to separate it from related compounds (20, 28, 31, 35). In terms of sequestration, it was demonstrated decades ago that monarchs preferentially sequester two cardenolides, calotropin and calactin, especially when feeding on *A. curassavica* (20, 31, 33, 36). For oviposition, two flavonol glycosides were isolated from *A. curassavica* leaves that stimulate egg laying (37). Nonetheless, the relative importance of quercetin glycosides versus cardenolides in oviposition is unknown, and specific cardenolides that impact larval growth and sequestration have not been well-studied. If *A. curassavica* defends itself against this specialized herbivore in a coevolutionary interaction mediated by plant chemistry, connecting specific toxins to their target site in the context of sequestration and oviposition is critical. In particular, we hypothesized that specific cardenolides modulate a trade-off between benefits of specialization and costs of coping with toxicity.

Here we identify cardenolides produced by *A. curassavica* and address which compounds are sequestered by monarchs, followed by asking four questions: 1) Do specific cardenolides reduce monarch larval growth or does sequestration impose a burden for larvae? 2) Using *in vivo* and *in vitro* assays, do monarchs detoxify or convert particular cardenolides to less toxic forms? 3) What is the relative toxicity (measured as *in vitro* inhibition of the cellular target, the monarch's Na^+/K^+ -ATPase) of non-sequestered cardenolides, those sequestered intact, and those modified during sequestration? And finally, 4) do monarch oviposition decisions minimize toxicity and optimize sequestration of cardenolides, or are oviposition stimulants (flavonol glycosides) drivers of oviposition?

Results

Plant cardenolides, sequestration, and conversion

Among the >200 *A. curassavica* plants grown in a common environment, the range of total leaf cardenolides varied 8-fold (0.96 – 8.16 mg/g dry mass). Of the nine cardenolides quantified, one apolar compound, thiazolidine ring-containing voruscharin, identified by liquid chromatography coupled with high resolution mass spectrometry (LC-HRMS/MS) was, on average, 40% of the total leaf cardenolides. Three other major peaks represented about 10%

each of the total (two unidentified compounds at retention times 14.7 and 17.9 minutes, and uscharin). Of the 36 pairwise phenotypic correlations between the nine cardenolides (n=212), all but four were highly significant and positive, and the four exceptions all involved voruscharin (Table S1). A principal components analysis (PCA) yielded two orthogonal PC axes explaining 85% of the variation in the concentrations of the nine cardenolides, with PC1 having loadings of over 0.5 for all peaks except voruscharin, while voruscharin dominated PC2 (Table S2). Thus, voruscharin production appears to be regulated somewhat independently from other *A. curassavica* cardenolides.

Monarch caterpillars were grown individually on these intact plants and were collected in their fourth instar, weighed, freeze dried, and had their guts removed. Chemical analysis by UV and mass spectrometry revealed an absence of voruscharin from caterpillar bodies (Figures 1A, S1, S2). Three compounds frugoside, calotropin and calactin accounted for 77% of the total sequestered cardenolides (Table S2). While frugoside occurred in both plant and insect tissues, calactin was very low in leaves, and calotropin, if present, was too low to quantify in leaves. The six other compounds sequestered were minor (each <6.5% of the total) and were not found in the plant.

To test if monarchs convert voruscharin to calactin and calotropin, we purified voruscharin from *A. curassavica*, painted it on leaves of *A. tuberosa* (a milkweed that is eaten by monarchs in nature but lacks cardenolides), and fed it to monarch caterpillars. In particular, we compared monarchs fed painted versus unpainted *A. tuberosa*, in addition to their frass and positive controls fed *A. curassavica*. First, an untargeted MS-based metabolomics analysis showed that the chemical compositions of the groups assessed by PERMANOVA were different ($P < 0.05$), although not all pairwise comparisons were significant (Figure 1A, Table S3). Second, in parallel, cardenolide sequestration was assessed by measuring absolute concentrations based on UV detection (Fig. 1B) and the relative concentrations based on LC-HRMS detection (Fig. S2). Voruscharin was only recovered on painted leaves, and in small quantities in caterpillar frass. Monarchs fed control *A. tuberosa* leaves lacked cardenolides and those fed painted leaves only contained calactin and calotropin. Finally, as expected, our positive control of monarchs fed *A. curassavica* foliage sequestered calactin and calotropin, in addition to several polar cardenolides, but lacked voruscharin.

To connect the dots of voruscharin synthesis and degradation, we hypothesized a biochemical model (Fig. S3) and examined transformation dynamics of voruscharin *in vivo* and *in vitro*. In particular, we hypothesized that voruscharin first degrades to uscharidin, which is secondarily converted to calactin and calotropin. We detected low levels of uscharidin in monarchs on *A. curassavica*, but uscharidin was absent in monarchs fed *A. tuberosa* painted with voruscharin and was found in traces in their frass (Fig. S4). To understand the degradation pathway, we conducted an assay in which pure voruscharin was subjected to different basic pH values and temperatures (Fig S5). Voruscharin is transformed to uscharidin under various alkaline conditions (pH 7-10) and the rate of conversion was enhanced at warmer temperatures (Fig. S5).

The burden of cardenolide consumption and sequestration

Although both plant cardenolide PC axes were associated with total plant cardenolide concentrations (Table S2), only PC2 (as well as the single compound voruscharin) predicted total cardenolides sequestered by monarchs (PC1 $F_{1,68}=0.296$, $p=0.588$, PC2 $F_{1,68}=5.501$, $p=0.022$, voruscharin $F_{1,68}=10.107$, $p=0.002$, Figure 2a). To address the relative importance of voruscharin (as a plant toxin) or sequestered cardenolides (as a burden, i.e., the combined effect of converting cardenolides and storing the preferred compounds), we used these two predictors in multiple regression to predict caterpillar growth (the two variables are only modestly correlated, $r=0.36$, variance inflation factor = 1.15). Here, monarch growth was strongly negatively predicted by total sequestered cardenolides ($R^2=0.61$), but not leaf voruscharin concentration (Figure 2b, sequestered cardenolide $F_{1,67}=85.660$, $p<0.001$, voruscharin $F_{1,67}=1.254$, $p=0.267$, Fig. S6). This analysis was robust to different configurations of using plant and sequestered cardenolides as predictors of monarch growth (i.e., using plant PC2 or total plant cardenolides and insect PC1 in multiple regressions, Fig. S6).

To address the inhibitory capacity of different cardenolides on their physiological target, the monarch Na^+/K^+ -ATPase, we isolated and purified frugoside (polar, sequestered intact), uscharin (apolar, 3-thiazoline ring-containing, minor leaf component, not sequestered), voruscharin (apolar, thiazolidine ring-containing, dominant leaf component, not sequestered), calotropin (intermediate polarity, minimal in the plant but sequestered), and calactin (intermediate polarity, minimal in the plant but sequestered) (Figs. S7-9). The inhibitory capacity of these compounds was referenced to two standards (ouabain and digitoxin) and all were compared on the sensitive porcine Na^+/K^+ -ATPase versus the highly resistant enzyme isolated from monarch neural tissues. The two non-sequestered cardenolides were the most potent inhibitors of the monarch Na^+/K^+ -ATPase and yet were among the least inhibitive of the sensitive porcine Na^+/K^+ -ATPase (Fig. 3). In particular, the monarch's Na^+/K^+ -ATPase is typically 50-100 times more resistant to cardenolides than the porcine Na^+/K^+ -ATPase (22, 38), and this was borne out by the average of 86-fold higher IC_{50} for five compounds tested, including 3 sequestered cardenolides and the two standards (Table S4; Figure 3). Strikingly, for non-sequestered uscharin and voruscharin, the monarch was less than 2-fold more resistant than the sensitive Na^+/K^+ -ATPase.

Monarch oviposition

When we tested free-flying monarchs for their oviposition preferences, egg laying was best predicted by intermediate concentrations of total leaf cardenolides and plant height (Figure 4, Poisson GLM: total cardenolides, L-R $\chi^2 = 5.638$, $p = 0.018$, total cardenolides squared L-R $\chi^2 = 4.827$, $p= 0.028$, and height L-R $\chi^2 = 15.395$, $p < 0.001$; alternative models including the significant predictive effect of cardenolide PC1 and individual compounds are given in Table S5). Neither leaf voruscharin nor plant PC2 predicted oviposition. Because egg laying was also not predicted by foliar concentrations of two quercetin glycosides in leaf tissues (a quercetin-

rhamno-di-hexoside and quercetin-rhamno-hexoside, Table S6, Fig. S10), we tested their stimulatory effect on oviposition by isolating and purifying the compounds. The latter compound was indeed found to be stimulatory in oviposition trials, but only at unrealistically high concentrations (Table S6). Thus, overall, oviposition on whole plants was best predicted by plant height and the set of more polar cardenolides which showed correlated expression, but neither the most potent cardenolides nor the low levels of quercetin glycosides in leaves.

Discussion

It has long-been conventional wisdom that specialist insect herbivores are less impacted by plant defensive chemistry than generalists; and reciprocally, specialist pests that have been persistent over millions of years are potent forces of natural selection for specific plant defenses (1, 2). Nonetheless, as Berenbaum et al. (7) pointed out over 30 years ago, there is potential for stalemate in the metaphorical coevolutionary arms race, where herbivores and plants are well-adapted to each other, with little room for further escalation. In the case of monarchs on milkweed, despite all the various barriers to feeding that milkweeds possess (trichomes, latex, and cardenolides), monarchs seem to prevail by shaving leaf trichomes and trenching latex canals as caterpillars, and possessing a highly cardenolide-insensitive sodium-potassium pump (13).

Here we have reported that the dominant cardenolide in one of the most important milkweed host plants for monarchs, the tropical milkweed *A. curassavica*, is the unusual thiazolidine ring-containing compound voruscharin. The fact that most cardenolides lack nitrogen and sulfur, and that nitrogen is typically limiting for plant growth, suggests that such compounds may be evolutionarily derived and highly potent (28). Although voruscharin has been known from *A. curassavica* and two other species in the Apocynaceae (*Gomphocarpus fruticosus* and *Calotropis procera*) for decades, and it was known not to be sequestered by monarchs, its potency, conversion, and impacts on sequestration and oviposition were largely unknown (20, 28, 31, 33, 35). We have found that voruscharin is among the most potent milkweed cardenolides known to inhibit the monarch Na^+/K^+ -ATPase (22), but it has rather poor inhibition of the highly sensitive porcine Na^+/K^+ -ATPase, suggesting that this compound and its high expression in *A. curassavica* may function specifically against the monarch butterfly. In related work, we will show that natural populations of *A. curassavica* harbor substantial genetic variation in voruscharin production.

In perhaps the best known system of plant-herbivore chemical coevolution, Berenbaum and colleagues (3) revealed how toxic furanocoumarins evolved in plants of the Apiaceae and the means by which lepidopteran herbivores detoxify these compounds. In particular, diverse cytochrome P450 enzymes in insects appear to have specifically evolved to detoxify the compounds. Among swallowtail butterflies, although linear furanocoumarins are metabolized easily, the biochemically novel angular furanocoumarins are much more challenging and have imposed selection to diversify cytochrome P450 enzymes. In the monarch – milkweed system, selective sequestration of more polar compounds is well-known, but metabolic detoxification

was thought to be far less important, in part because butterflies store cardenolides for their own defense (20, 24, 25). While some cardenolides like frugoside are stored intact, others such as voruscharin are converted to other forms. We found that the preferentially sequestered calactin and calotropin were less toxic to monarchs than voruscharin, but conversion or storage imposed a significant burden for caterpillars in terms of reduced growth rate that was stronger than direct effects of voruscharin itself. Ultimately the benefits of sequestering calactin and calotropin may outweigh the costs we have described here. Recent research indicates substantial genetic variation in monarchs for sequestration (15) and our future work will address selection on this ability.

It is interesting to note that the basic conditions which mimic the pH of the monarch gut hydrolyze voruscharin or uscharin to uscharidin. Our data support this as the first step in the hypothesized pathway to derive calactin and calotropin (Fig. S5). Acid hydrolysis of the 3-thiazoline ring has also been reported for the conversion of uscharin into uscharidin (28), and the enzymatic reduction of uscharidin to calactin and calotropin was demonstrated *in vivo* using monarch gut homogenates (20, 27). Perhaps it seems odd that a novel and highly potent chemical defense produced by *Asclepias* is degraded passively in the monarch gut. One possible explanation for this observation is that the degradation is not immediate and the further enzymatic modification is costly. Depending on the hydrolysis rate and temperature in the gut, all of the voruscharin may not be converted to uscharidin, potentially imposing a cost for monarchs. Spontaneous and environment-dependent degradation of plant defense compounds is not unique to cardenolides, and has been shown to have various effects in other systems (39-41).

Given the high chemical diversity of hundreds of distinct cardenolides in *Asclepias* (42), it is puzzling that very few cardenolides containing a 3-thiazoline or 3-thiazolidine ring have been found (e.g., uscharin, voruscharin, and labriformin) (28, 43). So far these have been found in some of the major host plants of monarchs, as labriformin occurs in *A. syriaca* (44), but the evolutionary history of these compounds and why they are not more common is thus far unclear. Although the biosynthesis of cardenolides in *Asclepias* has been little-studied (45), and the pathway leading to voruscharin in particular is unknown, we speculated that formation of the thiazolidine ring likely involves the condensation of cysteine with the carbonyl group in position 3' of uscharidin (Fig. S3). Regardless of the specific biosynthetic origin, our analysis of correlations among cardenolides (Table S1) suggests the biosynthetic steps involved in the thiazolidine ring formation may be regulated independently from the pathways that produce the bulk of other *A. curassavica* cardenolides.

There has been a lack of clarity on the relative importance of flavonoid oviposition stimulants (quercetin glycosides) and cardenolides (which do not occur on the surface of milkweed leaves) for egg laying. On the one hand, monarchs tend to oviposit on intermediate cardenolide concentration plants (29, 30), yet on the other hand, there does not appear to be a consistent relationship between cardenolides and quercetin glycosides (46, 47). In the current study, although we were able to show that an isolated quercetin-rhamno-hexoside was indeed

stimulatory for oviposition, quantitative variation in quercetin glycosides measured in leaves did not predict egg laying in our trials. We speculate that quercetin glycosides, although stimulatory in isolation, occur in much too low concentrations to be drivers of egg laying. Nonetheless, we did find that monarchs laid the most eggs on intermediate cardenolide plants as expected based on past observations. Our plants were not flowering during the oviposition trial, so nectar was not a potential cue, although other research indicates that nectar cardenolides impact monarch oviposition (48).

Finally, although we do not know how monarchs sense leaf cardenolides (or what correlated traits they detect), monarchs' preference for intermediate cardenolide plants supports the notion that specialist herbivores must balance the benefits of plant secondary compounds for sequestration with the burden that these same compounds impose. Thus, perhaps there is room for additional coevolution between these highly adapted herbivores and their toxic host plants. One challenge for monarchs is that there is relatively little evidence of local population differentiation or adaptation to particular host plants (14, 15). This is likely the outcome of their complex annual migratory cycle, where butterflies encounter diverse milkweeds and yet geographically distinct breeding populations intermix during migration and overwintering. Thus, although monarchs themselves are specialists on a genus of plants, that genus contains chemically diverse cardenolide toxins for which there may not be a single insect counter-ploy (28, 49). In fact, recent work has also shown that alternative defenses may result in some plants being ecological traps where monarch oviposition is followed by poor caterpillar performance (9, 50). Thus, we conclude by speculating that although monarchs are highly adapted to *Asclepias* spp. overall, they may not be able to strongly adapt to any one plant species. The ratio of cardenolide sequestration by monarchs to host plant cardenolides is the highest for *A. syriaca* and *A. curassavica* (24), suggesting that coevolution may be primarily occurring between monarchs and these two species. And strong selection by monarchs on particularly important host plant species (e.g., *A. syriaca* and *A. curassavica*) may stimulate adaptation in these plant species. Thus, coevolution in this system is decidedly diffuse. The geographical availability of multiple milkweed species is a buffet for monarchs, but perhaps also a limitation preventing stronger specialized insect adaptation.

Materials and methods

Plant growth

In April 2016 we germinated a diverse pool of *Asclepias curassavica* seeds, collected from several sites in the southern USA, Mexico, and obtained from commercial seed suppliers. Our goal was to have diversity within the species, and there was substantial phenotypic variation among collections (e.g., in flower color and leaf shape), but all were confirmed to be *A. curassavica* based on flowers. In total, we grew approximately ten plants were from each of 22 collections. Plants were grown as described in Rasmann and Agrawal (49), with surface-sterilized seeds that were nicked, stratified at 4 °C for four days, germinated in petri dishes at

28 °C, grown in potting soil (Metro-Mix, Sun Gro Horticulture) in plastic pots (500 ml) in a high light growth chamber (at least 350 microeinsteins, 16 h daylight, 26 °C day : 22 °C night). Plants were given two applications of dilute fertilizer (N:P:K 21:5:20, 150 ppm N [$\mu\text{g/g}$]) over one month of growth, after which they were clipped to just above the cotyledons. Clipped leaf tissue was freeze-dried and analyzed for cardenolides by HPLC (see below). Plants were up-potted and moved to a rooftop greenhouse at Cornell University. A total of 212 *A. curassavica* plants regrew in the greenhouse.

Initial insect bioassays

Two assays were conducted. In the first, adult oviposition was assessed by releasing 10 mated female monarchs (from a laboratory colony) into the 56 m² greenhouse. After 24 hours, over one third of the plants had at least one egg laid on them and the trial was ended. Plant height was measured, eggs were removed from plants with tweezers, and the second assay was initiated to assess caterpillar growth. Neonate monarch caterpillars were introduced to 70 of the plants and growth rate was measured as fresh mass eight days later when the caterpillars had entered the fourth instar (when monarchs typically begin to move between plants). Caterpillars were freeze-dried, their guts were removed by dissection under a microscope, and the rest of the body was used to assess cardenolide sequestration. We then estimated the total cardenolides sequestered by HPLC (see below the cardenolide quantification). This design allowed us to connect individual variation in plant chemistry, caterpillar growth, and sequestration.

Cardenolides and flavonols isolation and identification

We authenticated chemical structures using a set of authentic standards from Zhang et al. (51) and Petschenka et al. (22) and matched retention times, mass spectrometry exact masses (HRMS) and MS fragmentation profiles for frugoside, asclepin, calactin, calotropin in samples, and for purified compounds voruscharin, uscharin, and two flavonols quercetin-rhamno-hexoside and quercetin-rhamno-di-hexoside. HRMS/MS data of voruscharin, uscharidin, calactin and calotropin are detailed in Table S7 and their respective MS² can be found in Fig. S7-S9. Fig. S10-S11 give the HRMS/MS data for the quercetin glycosides.

Frugoside, calactin, and calotropin were purified from the bioassay monarch caterpillars raised on *A. curassavica* (3.1 g dry tissue with the guts). The pooled extract was de-fatted with 50mL hexane and taken to dryness. The remaining residue was suspended in 9mL of 16% acetonitrile and water, sonicated for 30sec, vortexed, centrifuged at 20,800g for 12min and treated by adding 24uL of 40% lead acetate. This step clears the sample of pigments and other interfering compounds. The vial was then lightly vortexed and allowed to sit for a minimum of 10min to allow unwanted compounds to complex. The vial was then centrifuged at 20,800g for 12min and the supernatant transferred to a new vial. To bind up any remaining lead ions, we

added an addition of 1200uL of 5% sodium sulfate. After a 10min wait, the vial was again centrifuged at 20,800g for 12min and the supernatants transferred to a new vial. The vial was then taken to dryness and the residue re-suspended in 9mL of methanol by sonication and vortexing. The vial was then centrifuged at 20,800g for 12min and the supernatant transferred to a new vial. The methanolic supernatant was transferred to a new vial and taken to dryness. We then added 16% acetonitrile to water and the residue was re-suspended by sonication and vortexing. The sample was again centrifuged at 20,800g for 12min and the supernatant saved for preparative HPLC fractionation. Uscharin and voruscharin were purified from >40mL of fresh *A. curassavica* latex collected from greenhouse grown plants.

All prepared samples were injected into an Agilent 1260 series preparative LC system with an Agilent 21.2mm x 150mm, C-18, 5um column. Each first-pass injection was eluted at a constant flow rate of 14.87mL/min with a gradient of acetonitrile and water as follows: 0-2min at 16% acetonitrile; 2-25min from 16% to 70%; 25-30min from 70% to 95%; 30-35min at 95%. Target peaks were detected at 218nm. In most cases, each first-pass target fraction needed to be dried down, re-suspended in 16% acetonitrile and re-injected for further cleanup. Fractions needing re-injection often required modifications to the Method gradients to increase column retention times to help isolate target peaks. The isolated fractions were pooled, dried, and re-suspended in 0.5 ml of 100% MeOH, and then analyzed on a Thermo Scientific QExactive™ hybrid quadrupole-orbitrap LC-MS system in positive ionization mode (see below the LC-HRMS instrument parameters). Compounds were identified by their exact parental mass ($[M+H]^+$), as well as the corresponding sodium adduct ($[M+Na]^+$).

Reversed-phase chromatography was performed using a Dionex 3000 LC coupled to an Orbitrap Q-Exactive mass spectrometer controlled by Xcalibur software (ThermoFisher Scientific). Methanolic extracts were separated on an Agilent Zorbax Eclipse XDB-C18 column (150 mm x 2.1 mm, particle size 1.8 μ m) maintained at 40 °C with a flow rate of 0.5 mL/min. Solvent A: 0.1% formic acid (FA) in water; solvent B: 0.1% formic acid in acetonitrile. A/B gradient started at 5% B for 2 min after injection and increased linearly to 98% B at 11 min, followed by 3 min at 98% B, then back to 5% B over 0.1 min and finally at 5% B held for an additional 2.9 min to re-equilibrate the column. Mass spectrometer parameters: spray voltage (-3.0 kV, +3.5 kV), capillary temperature 380 °C, probe heater temperature 400 °C; sheath, auxiliary, and sweep gas 60, 20, and 2 AU, respectively. S-Lens RF level: 50, resolution 240,000 at m/z 200, AGC target 3E6. Each sample was analyzed in negative and positive electrospray ionization modes with m/z ranges 70-1000 for reversed-phase, 120-800 for reversed-phase post-column ion pairing, and 70-700 for normal-phase. Parameters for MS/MS (dd-MS2): MS1 resolution: 60,000, AGC Target: 1E6. MS2 resolution: 30,000, AGC Target: 2E5, maximum injection time: 50 msec, isolation window 1.0 m/z , stepped normalized collision energy (NCE) 10, 30; dynamic exclusion: 1.5 seconds, top 5 masses selected for MS/MS per scan. LC-MS data

were analyzed using MZmine software (see below) and MS² spectra were obtained via Excalibur software (ThermoFisher Scientific).

Cardenolide and flavonol quantification

We used an Agilent 1100 HPLC with diode array detector and a Gemini C18 reversed-phase, 3 μ m, 150 mm x 4.6 mm column. We use 50 mg of pulverized tissue for analyses by adding 1.5 ml of 100% methanol, a 20 μ g digitoxin spike as internal standard, and 20 FastPrep beads. Cardenolides were then extracted by agitating twice on a FastPrep-24 homogenizer for 45 s at 6.5 m/s and then centrifuged at 20,800 g for 12 min. Supernatants were dried down in a vacuum concentrator at 35C and were resuspended in 200ul methanol, filtered using 0.45 μ m hydrophilic membranes, and 15ul was inject into the HPLC running a constant flow of 0.7 ml/min with a gradient of acetonitrile and water as follows: 0–2 min at 16% acetonitrile; 2–25 min from 16% to 70%; 25–30 min from 70% to 95%; 30–35 min at 95%; followed by 10 min reconditioning at 16% acetonitrile. Peaks were recorded at 218 nm and absorbance spectra are recorded between 200 nm to 300 nm. Peaks showing a characteristic single absorption maximum between 214 and 222 nm correspond to the unsaturated lactone indicative of cardenolides. Concentrations were standardized by peak area to the digitoxin internal standard with known concentration. Flavonols were similarly quantified from the same chromatograms based on our digitoxin internal standard.

Voruscharin painting experiment

We modeled our analysis of the fate of purified cardenolides based on Seiber et al. (20). We used monarchs from a laboratory colony (reared for 4 generations from wild collected individuals) and reared a cohort on *A. tuberosa*. *A. tuberosa* is milkweed that lacks detectable cardenolides and has the lowest inhibition of the porcine sodium-potassium pump of any milkweed species assayed to date (52). When caterpillars newly molted to the 4th instar, we kept them cool and without food until use (<5 hours). Our main treatments were *A. tuberosa* leaves (controls treated with methanol, n=5) and leaves dosed with realistic amounts of voruscharin (n=4). Briefly, because voruscharin was estimated to be 40% of total cardenolides in *A. curassavica* and totals an average of 1.7 μ g/mg dry mass, we added 7 μ g of voruscharin (dissolved in methanol) per cm² of *A. tuberosa* foliage. Individual caterpillars were provided two leaves at a time in petri dishes lined with filter paper. After molting into 5th instar, they were deprived of food for 8 hours and freeze-dried for analysis. Two caterpillars were simultaneously reared on *A. curassavica* from hatching to the 5th instar. In addition to these positive controls, we analyzed samples from methanol treated *A. tuberosa* leaves, *A. tuberosa* leaves spiked with voruscharin, caterpillars fed each of these diets, and the frass from caterpillars fed the voruscharin diet.

Oviposition experiments

We modeled oviposition trials with isolated quercetin glycosides on Haribal and Renwick (37). Briefly, cubes of washed green sponges were arranged on a four-arm stand inside of a

collapsible field cage (Bioquip, 0.23 m³). Each trial consisted of two control arms (sponge with water) and one sponge each of the two isolated quercetin glycosides (1 gram leaf equivalents); at least 4 female (all mated) and 1 male butterflies were included in each of 10 trials. Butterflies were allowed to lay eggs for a maximum of 5 hours (daylight hours). All eggs were counted on sponges for analysis.

Data pre-processing and metabolomics analysis

The acquired LC-MS data files were converted to mzXML files using the ProteoWizard MSconvert tool. LC-MS data was then preprocessed with the open-source MZmine software and consisted of peak detection, removal of isotopes, alignment, filtering, and peak filling. Peak detection was performed in three steps: (i) mass detection with noise value = 15,000; (ii) ADAP chromatogram builder with minimum group size in number of scan = 5, group intensity threshold = 25,000, minimum height = 30,000 and m/z tolerance = 10 ppm; (iii) wavelets ADAP deconvolution with S/N = 3, minimum feature height = 1,000, coefficient area threshold = 5, peak duration range = 0.01–3 min, retention time wavelet range = 0.01–0.04 min. Isotopes were removed using the isotopic peak grouper with m/z tolerance = 10 ppm, retention time tolerance = 0.5 min, maximum charge = 3. Chromatograms were aligned using the join aligner with m/z tolerance = 10 ppm, weight for m/z = 75, retention time tolerance = 0.5 min, weight for retention time = 25. Filtering minimum peak in a row = 2, minimum peak in an isotopic pattern = 2, and keep only peaks with MS2 scan. Gap filling was applied using the method peak finder with retention time correction with intensity tolerance = 10%, m/z tolerance = 10 ppm, retention time tolerance = 0.5 min. Quality control (QC) metabolites with a coefficient of variation (CV) greater than 30% were removed from the whole data matrix. In positive mode ionization the data matrices contain 7,252 and 6,795 features in mass range of 152–1185 m/z and 156–1155 m/z respectively.

Sodium-potassium pump assays

We quantified the biological activity of isolated cardenolides using Na⁺/K⁺-ATPase from the porcine cerebral cortex (Sigma-Aldrich, MO, USA) and monarch butterflies following methods of Petschenka et al. (22). Briefly, Na⁺/K⁺-ATPase activity was measured as the amount of inorganic phosphate (Pi) enzymatically released from ATP in the presence of K⁺ (Na⁺/K⁺-ATPase active) minus the amount of Pi released in the absence of K⁺ (Na⁺/K⁺-ATPase inactive). Each compound was dissolved fully in methanol (frugoside, calactin, and calotropin) or acetonitrile (voruscharin and uscharin, due to solubility), assayed by HPLC to determine concentration, and then dried and resuspended in 20% DMSO to a concentration of either 0.5mM (frugoside, calactin, and calotropin) or 0.1mM (voruscharin and uscharin, due to decreased solubility). We then prepared five serial dilutions to reach the following concentrations: 5x10⁻⁵M, 5x10⁻⁶M, 5x10⁻⁷M, 5x10⁻⁸M, 5x10⁻⁹M, to produce a six-point inhibition curve for each compound, incubated with each of the two enzyme preparations. These milkweed cardenolides were run alongside equivalent solutions of ouabain and digitoxin in 20%

DMSO. Reactions were performed in 96-well microplates on a BioShake Iq microplate shaker (Quantifoil Instruments, Jena, Germany) at 200 rpm and 37 °C. Absorbance values of reactions were corrected by their respective backgrounds and dose-response curves were fitted using a non-linear mixed effects model with a 4-parameter logistic function in the statistical software R (function *nlme* with *SSfpl* in package *nlme* v3.1–137) based on ref (53). We focus analyses on the dilution value IC50 at which the enzyme is inhibited by 50%.

Statistical approaches

Linear statistical models (regression, ANOVA) were usable for most analyses and residuals were checked for normality and heteroscedasticity. Except as noted below, all analyses were conducted in JMP Pro V14. As noted in the text, we quantified nine abundant cardenolides in the leaf tissue of *A. curassavica* and nine sequestered cardenolides in monarchs (which overlapped but were not identical to those in plants). As shown in the results, the concentrations of many, but not all, of the distinct cardenolides were highly correlated across individual plants. We thus first used principal components analysis to reduce the number of variables in each set and used the two PCs (eigenvalues >1) in statistical analyses (mostly regressions to explain response variables like egg number, larval mass, and sequestration). Next, to confirm a role (or lack thereof) for particular cardenolides that were strongly (or weakly) loaded on particular PC axes, we followed up with analyses using the individual compounds.

Metabolomic analyses were performed using the web-based metabolomics data processing tool MetaboAnalyst 3.0 (<http://www.metaboanalyst.ca/>). Briefly data were filtered using a non-parametric relative standard deviation (MAD/medium), normalized by sum, log transformed and auto scaled. The metabolomes of each group of samples were analyzed with a Bray–Curtis distance matrix on normalized chemical data and visualized using principal coordinates analyses (PCoA). Statistical tests were conducted using PERMANOVA.

We used a Poisson regression to predict egg count data which ranged from 0-6 eggs per plant; a squared term was included in the model both because past work (29, 30) and the current results fit a quadratic model.

Acknowledgements

We thank Bennett Fox and Frank Schroeder for unfailing assistance with the mass spectrometry of cardenolides at the Boyce Thompson Institute and Nicolas Baert for mass spectrometry analyses of quercetin glycosides at the Cornell Chemical Ecology Core Facility. Chelsea Lee and Steven Broyles helped with latex collection. The manuscript was improved by comments from two anonymous reviewers, Nathaniel Carlson, Tyler Coverdale, Arielle Johnson, Xosé López-Goldar, Jennifer Thaler and Shirley Zhang. Frances Fawcett drew the monarch in the figures. **Funding:** This research was supported by a grant from the National Science Foundation to A.A.A. (IOS-1907491). **Author contributions:** K.B. conducted the plant grow up, monarch bioassays on whole plants, and plant HPLC-UV analysis. M.H. helped with the quantification,

isolation, and identification of the quercetin glycosides. A.P.H. supported most of the experiments and conducted all sodium-potassium pump assays. R.A.W. conducted caterpillar sequestration analyses on HPLC-UV and isolated the cardenolides. R-W.J. provided cardenolide standards. C.D. conducted the LC-HRMS analysis of cardenolides, analyzed the metabolomics data, designed and performed the voruscharin degradation experiment, and proposed the biosynthetic pathways. A.A.A. designed the research, conducted the monarch bioassays on purified compounds, and wrote the manuscript (all authors contributed to the writing and editing). **Competing interests:** The authors declare no competing financial and non-financial competing interests. **Data and materials availability:** All data is available in the main text or in the supplementary materials.

Supplementary Materials:

Figures S1-S11

Tables S1-S7

References

1. Cornell HV & Hawkins BA (2003) Herbivore responses to plant secondary compounds: A test of phytochemical coevolution theory. *Am. Nat.* 161(4):507-522.
2. Rothwell EM & Holeski LM (2019) Phytochemical defences and performance of specialist and generalist herbivores: a meta-analysis. *Ecol. Entomol.*:doi.org/10.1111/een.12809.
3. Berenbaum MR (2002) Postgenomic chemical ecology: from genetic code to ecological interactions. *J. Chem. Ecol.* 28(5):873-896.
4. Renwick JAA, Haribal M, Gouinguéné S, & Städler E (2006) Isothiocyanates stimulating oviposition by the diamondback moth, *Plutella xylostella*. *J. Chem. Ecol.* 32(4):755-766.
5. Nieminen M, Suomi J, Van Nouhuys S, Sauri P, & Riekkola M-L (2003) Effect of iridoid glycoside content on oviposition host plant choice and parasitism in a specialist herbivore. *Journal of Chemical Ecology* 29(4):823-844.
6. Heisswolf A, Obermaier E, & Poethke HJ (2005) Selection of large host plants for oviposition by a monophagous leaf beetle: nutritional quality or enemy-free space? *Ecol. Entomol.* 30(3):299-306.
7. Berenbaum MR, Zangerl AR, & Nitao JK (1986) Constraints on chemical coevolution: wild parsnips and the parsnip webworm. *Evolution* 40:1215-1228.
8. Scheirs J, De Bruyn L, & Verhagen R (2000) Optimization of adult performance determines host choice in a grass miner. *Proc. R. Soc. Lond. Ser. B-Biol. Sci.* 267(1457):2065-2069.
9. Jones PL & Agrawal AA (2019) Beyond preference and performance: host plant selection by monarch butterflies, *Danaus plexippus*. *Oikos* 128:1092-1102.
10. Gripenberg S, Mayhew PJ, Parnell M, & Roslin T (2010) A meta-analysis of preference–performance relationships in phytophagous insects. *Ecol. Lett.* 13(3):383-393.
11. Thompson J (2005) *The Geographic Mosaic of Coevolution* (University of Chicago Press, Chicago).
12. Zangerl AR & Berenbaum MR (2003) Phenotype matching in wild parsnip and parsnip webworms: Causes and consequences. *Evolution* 57(4):806-815.
13. Agrawal AA (2017) *Monarchs and milkweed: A migrating butterfly, a poisonous plant, and their remarkable story of coevolution* (Princeton University Press, Princeton, NJ) p 296.
14. Zhan S, *et al.* (2014) The genetics of monarch butterfly migration and warning colouration. *Nature* 514(7522):317-321.
15. Freedman MG, Jason C, Ramírez SR, & Strauss SY (2020) Host plant adaptation during contemporary range expansion in the monarch butterfly. *Evolution* 74(2):377-391.
16. Brower LP & Moffitt CM (1974) Palatability dynamics of cardenolides in monarch butterfly. *Nature* 249(5454):280-283.
17. Agrawal AA (2005) Natural selection on common milkweed (*Asclepias syriaca*) by a community of specialized insect herbivores. *Evol. Ecol. Res.* 7:651-667.

18. Zalucki MP, Brower LP, & Alonso A (2001) Detrimental effects of latex and cardiac glycosides on survival and growth of first-instar monarch butterfly larvae *Danaus plexippus* feeding on the sandhill milkweed *Asclepias humistrata*. *Ecol. Entomol.* 26(2):212-224.
19. Rasmann S, Johnson MD, & Agrawal AA (2009) Induced responses to herbivory and jasmonate in three milkweed species. *J. Chem. Ecol.* 35(11):1326-1334.
20. Seiber JN, Tuskes PM, Brower LP, & Nelson CJ (1980) Pharmacodynamics of some individual milkweed cardenolides fed to larvae of the monarch butterfly (*Danaus plexippus* L.). *J. Chem. Ecol.* 6(2):321-339.
21. Agrawal AA, Ali JG, Rasmann S, & Fishbein M (2015) Macroevolutionary trends in the defense of milkweeds against monarchs: latex, cardenolides, and tolerance of herbivory. *Monarchs in a Changing World: Biology and Conservation of an Iconic Insect*, eds Oberhauser K, Altizer S, & Nail K (Cornell University Press, Ithaca, NY), pp 47-59.
22. Petschenka G, *et al.* (2018) Relative selectivity of plant cardenolides for Na⁺/K⁺-ATPases from the monarch butterfly and non-resistant insects. *Frontiers in Plant Science* 9:1424 (<https://doi.org/1410.3389/fpls.2018.01424>).
23. Nelson C (1993) A model for cardenolide and cardenolide glycoside storage by the monarch butterfly. *Biology and Conservation of the Monarch Butterfly, Los Angeles*, eds Zalucki MP & Malcolm SB), pp 83–90.
24. Malcolm SB (1995) Milkweeds, monarch butterflies and the ecological significance of cardenolides. *Chemoecology* 5/6:101-117.
25. Jones PL, Petschenka G, Flacht L, & Agrawal AA (2019) Cardenolide intake, sequestration, and excretion by the monarch butterfly along gradients of plant toxicity and larval ontogeny. *J. Chem. Ecol.* 45(3):264-277.
26. Frick C & Wink M (1995) Uptake and sequestration of ouabain and other cardiac glycosides in *Danaus plexippus* (Lepidoptera, Danaidae) - evidence for a carrier-mediated process. *J. Chem. Ecol.* 21(5):557-575.
27. Marty MA & Krieger RI (1984) Metabolism of uscharidin, a milkweed cardenolide, by tissue homogenates of monarch butterfly larvae, *Danaus plexippus* L. *J. Chem. Ecol.* 10(6):945-956.
28. Seiber JN, Lee SM, & Benson J (1983) Cardiac glycosides (cardenolides) in species of *Asclepias* (Asclepiadaceae). *Handbook of natural toxins* 1:43-83.
29. Oyeyele SO & Zalucki MP (1990) Cardiac glycosides and oviposition by *Danaus plexippus* on *Asclepias fruticosa* in south-east Queensland (Australia), with notes on the effect of plant nitrogen content. *Ecol. Entomol.* 15:177-186.
30. Zalucki MP, Brower LP, & Malcolm SB (1990) Oviposition by *Danaus plexippus* in relation to cardenolide content of three *Asclepias* species in the southeastern USA. *Ecol. Entomol.* 15:231-240.

31. Malcolm SB (1990) Chemical defence in chewing and sucking insect herbivores: plant-derived cardenolides in the monarch butterfly and oleander aphid. *Chemoecology* 1(1):12-21.
32. Zhang R-R, *et al.* (2014) Structures, chemotaxonomic significance, cytotoxic and Na⁺, K⁺-ATPase inhibitory activities of new cardenolides from *Asclepias curassavica*. *Organic Biomolecular Chemistry* 12(44):8919-8929.
33. Roeske C, Seiber J, Brower L, & Moffitt C (1976) Milkweed cardenolides and their comparative processing by monarch butterflies (*Danaus plexippus* L.). *Biochemical Interaction Between Plants and Insects*, (Springer), pp 93-167.
34. Faldyn MJ, Hunter MD, & Elderd BD (2018) Climate change and an invasive, tropical milkweed: An ecological trap for monarch butterflies. *Ecology* 99(5):1031-1038.
35. Hesse G & Ludwig G (1960) African arrow poisons XIV. Voruscharin, a second sulfur-containing heart poison from *Calotropis procera* L. . *Justus Liebigs Annalen der Chemie* 632:158-171.
36. Reichstein T, Von Euw J, Parsons JA, & Rothschild M (1968) Heart poisons in the monarch butterfly. *Science* 161(3844):861-866.
37. Haribal M & Renwick JAA (1996) Oviposition stimulants for the monarch butterfly: Flavonol glycosides from *Asclepias curassavica*. *Phytochemistry* 41(1):139-144.
38. Vaughan GL & Jungreis AM (1977) Insensitivity of lepidopteran tissues to ouabain - physiological mechanisms for protection from cardiac glycosides. *J. Insect Physiol.* 23(5):585-589.
39. Wouters FC, Blanchette B, Gershenzon J, & Vassão DG (2016) Plant defense and herbivore counter-defense: benzoxazinoids and insect herbivores. *Phytochemistry Reviews* 15(6):1127-1151.
40. Magalhães CP, Xavier-Filho J, & Campos FA (2000) Biochemical basis of the toxicity of manipueira (liquid extract of cassava roots) to nematodes and insects. *Phytochemical Analysis* 11(1):57-60.
41. Winde I & Wittstock U (2011) Insect herbivore counteradaptations to the plant glucosinolate–myrosinase system. *Phytochemistry* 72(13):1566-1575.
42. Agrawal AA, Petschenka G, Bingham RA, Weber MG, & Rasmann S (2012) Toxic cardenolides: chemical ecology and coevolution of specialized plant-herbivore interactions. *New Phytol.* 194(1):28-45.
43. Abe F & Yamauchi T (2000) An androstane bioside and 3'-thiazolidinone derivatives of doubly-linked cardenolide glycosides from the roots of *Asclepias tuberosa*. *Chemical & Pharmaceutical Bulletin* 48(7):991-993.
44. Malcolm SB, Cockrell BJ, & Brower LP (1989) Cardenolide fingerprint of monarch butterflies reared on common milkweed, *Asclepias syriaca* L. *J. Chem. Ecol.* 15(3):819-853.
45. Groeneveld HW, Binnekamp A, & Seykens D (1991) Cardenolide biosynthesis from acetate in *Asclepias curassavica*. *Phytochemistry* 30(8):2577-2585.

46. Agrawal AA, Salminen J-P, & Fishbein M (2009) Phylogenetic trends in phenolic metabolism of milkweeds (*Asclepias*): Evidence for escalation. *Evolution* 63:663–673.
47. Haribal M & Renwick JAA (1998) Identification and distribution of oviposition stimulants for monarch butterflies in hosts and nonhosts. *J. Chem. Ecol.* 24(5):891-904.
48. Jones PL & Agrawal AA (2016) Consequences of toxic secondary compounds in nectar for mutualist bees and antagonist butterflies. *Ecology* 97(10):2570-2579.
49. Rasmann S & Agrawal AA (2011) Latitudinal patterns in plant defense: evolution of cardenolides, their toxicity and induction following herbivory. *Ecol. Lett.* 14(5):476-483.
50. DiTommaso A & Losey JE (2003) Oviposition preference and larval performance of monarch butterflies (*Danaus plexippus*) on two invasive swallow-wort species. *Entomol. Exp. Appl.* 108(3):205-209.
51. Zhang R-R, *et al.* (2014) Structures, chemotaxonomic significance, cytotoxic and Na⁺, K⁺-ATPase inhibitory activities of new cardenolides from *Asclepias curassavica*. *J Organic Biomolecular Chemistry* 12(44):8919-8929.
52. Züst T, Petschenka G, Hastings AP, & Agrawal AA (2019) Toxicity of milkweed leaves and latex: chromatographic quantification versus biological activity of cardenolides in 16 *Asclepias* species. *J. Chem. Ecol.* 45(1):50-60.
53. Züst T, *et al.* (2020) Independent evolution of ancestral and novel defenses in a genus of toxic plants (*Erysimum*, Brassicaceae). *eLife* 9:e51712.

Figure legends

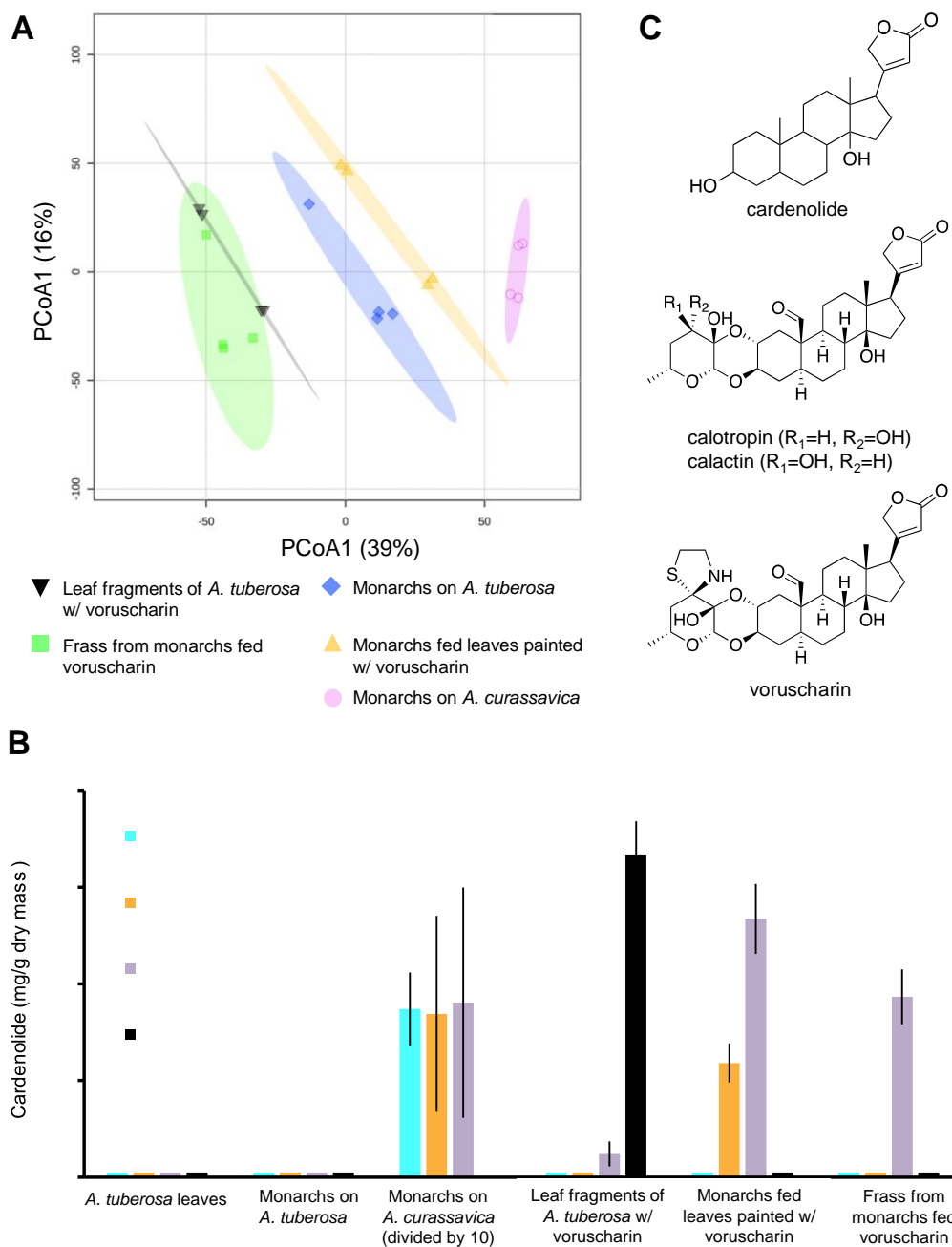


Fig. 1. Chemical conversion of milkweed cardenolides by monarch caterpillars. A) A visualization of metabolomic data showing the differences in the chemical composition across sample groups ($n=4$ per group, significance tested by PERMANOVA). After data curation over 7000 chemical features (m/z) were generated with MS data collected in positive ionization mode and

visualized with a Bray–Curtis distance matrix. Ellipses represent the region of 95% confidence. B) Voruscharin was converted to calactin and calotropin when fed to monarch caterpillars. Shown are means \pm SE concentrations as determined by UV-HPLC (n=3-9). Data bars very close to zero had no detectable cardenolides. Note that the caterpillars fed *A. curassavica* were reared on this diet from hatching and had an order of magnitude higher cardenolides than other treatments which were dosed only during the fourth instar. C) The basic skeleton of cardenolides and the chemical structures of calactin, calotropin, and voruscharin.

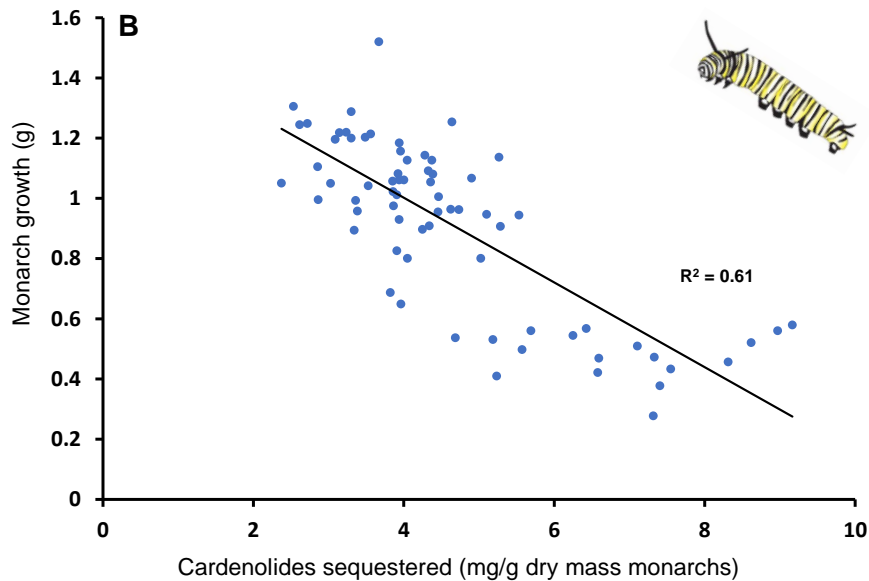
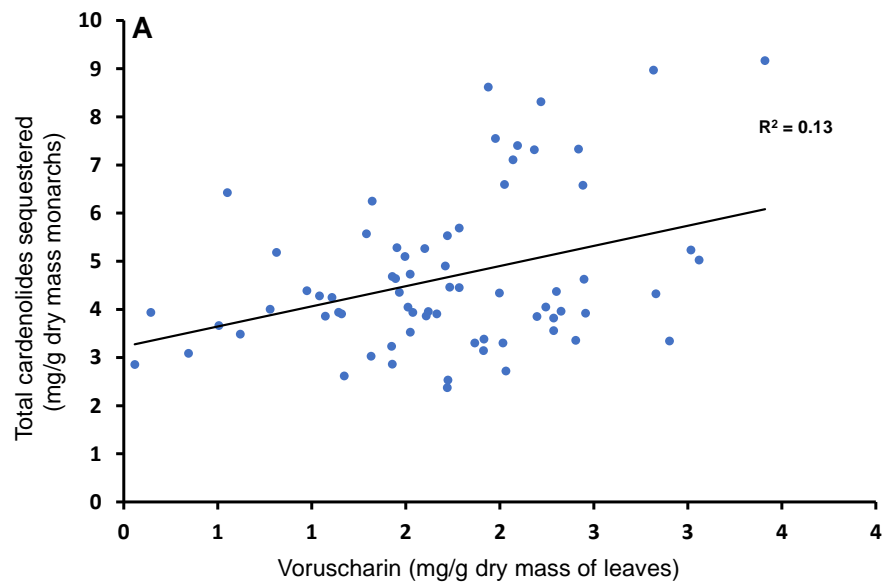


Fig. 2. Connections between plant cardenolides, monarch sequestration, and monarch growth. A) Sequestration was predicted by concentration of the dominant plant cardenolide, voruscharin, although this compound was itself not sequestered (it was converted to calactin and calotropin). B) In multiple regression, sequestered cardenolides were predictive of monarch growth (whereas plant cardenolides were not), indicating a cost of converting or storing cardenolides. The weak relationships of growth predicted by total leaf cardenolides and leaf voruscharin are shown in Fig. S6.

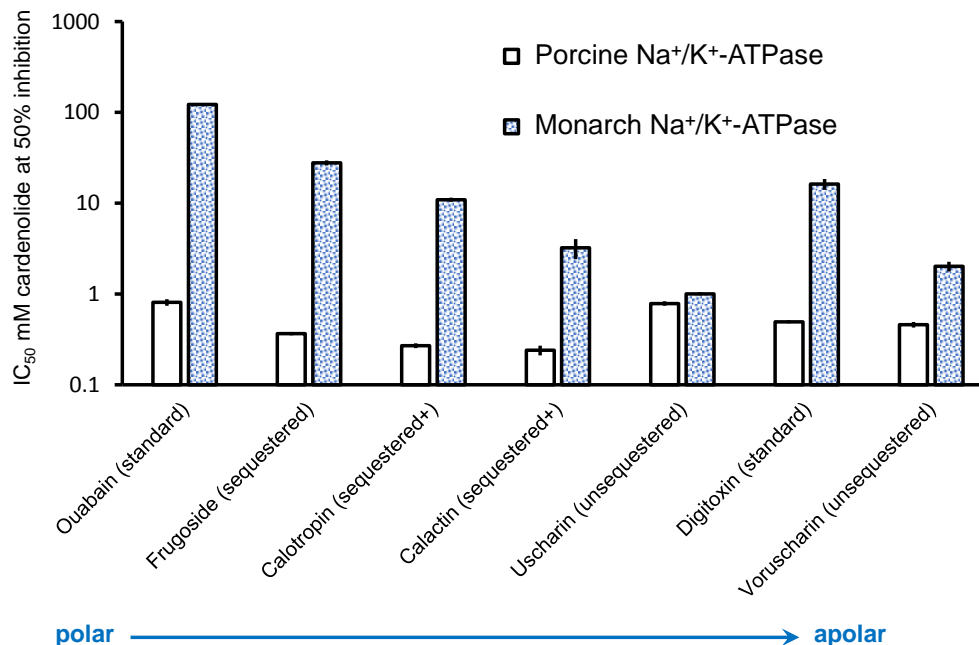


Fig.3. The difference in inhibitory impacts of isolated cardenolides on the highly sensitive porcine Na^+/K^+ -ATPase versus the milkweed-adapted monarch butterfly Na^+/K^+ -ATPase. Data are presented as the molar concentration of plant toxin necessary to cause 50% inhibition of the animal enzyme, or IC_{50} , on the Y axis. Thus, higher values on the log scale Y axis indicate that the enzyme is more resistant to the cardenolide. The monarch Na^+/K^+ -ATPase is substantially more resistant (it typically takes a higher concentration of the plant compounds to inhibit the enzyme). Sequestered+ indicates that these compounds are sequestered intact from consumed leaves as well as converted products from consumed voruscharin and uscharin. Each bar is a mean of 3-9 replicates (each based on a 6-concentration inhibition curve) \pm SE (where not visible, SEs are too small). The arrow representing the polarity of cardenolides is based on elution through a C18 HPLC column (apolar stationary phase).

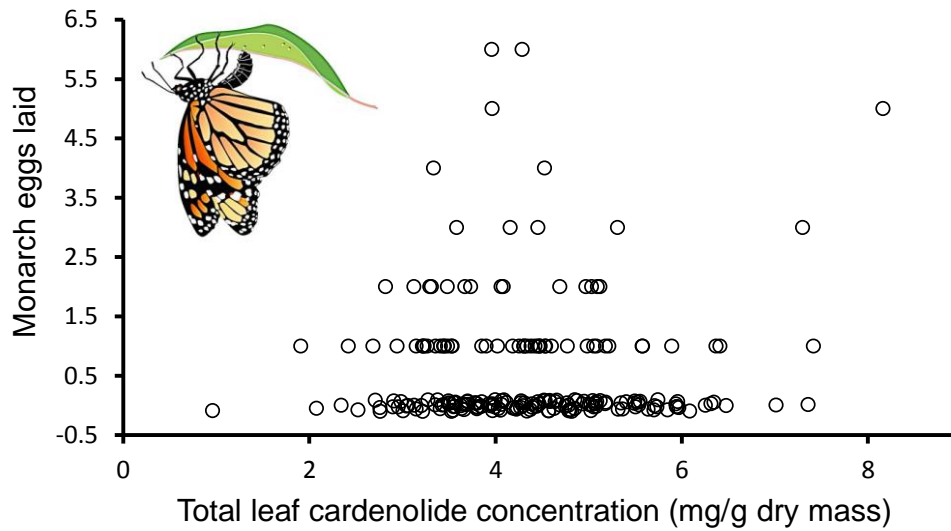


Fig. 4. Monarch oviposition was a quadratic function of total leaf cardenolides, with the highest number of eggs laid on intermediate cardenolide plants. Ten butterflies were released to freely oviposit in a large greenhouse common garden (n=212 plants). Although raw data are shown, plant height was included and was significant in the statistical model. Zero egg values have been jittered.

Supplementary Information for

Cardenolides, toxicity and the costs of sequestration in the coevolutionary interaction between monarchs and milkweeds

Anurag A. Agrawal^{1,2*}, Katalin Böröczky¹, Meena Haribal³, Amy P. Hastings¹, Ronald A. White¹
Ren-Wang Jiang⁴, Christophe Duplais⁵

Email: agrawal@cornell.edu

This PDF file includes:

Figures S1 to S11

Tables S1 to S7

References

Fig. S1. Sample HPLC chromatograms.	26
Fig. S2. Voruscharin painted on cardenolide-free milkweed leaves of <i>A. tuberosa</i> are converted to calactin and calotropin as revealed by LC-ESI- HRMS (n=4).	27
Fig. S3. Voruscharin putative biosynthesis in <i>Asclepias curassavica</i> and its degradation pathway in monarch gut.	28
Fig. S4. Uscharidin relative concentrations in samples.	29
Fig. S5. Voruscharin stability assay at different pH values.	30
Fig. S6. Monarch caterpillar growth predicted by A) total leaf cardenolide and B) leaf voruscharin concentrations.	32
Fig. S7. MS/MS product ion mass spectrum from [M+FA-H] ⁻ adduct of voruscharin.	34
Figure S8. MS/MS product ion mass spectrum from [M+FA-H] ⁻ adduct of uscharidin.	36
Figure S9. MS/MS product ion mass spectrum from [M+FA-H] ⁻ adduct of calotropin.	37
Figure S10. MS/MS product ion mass spectrum from [M+H] ⁺ adduct of quercetin-rhamno-hexoside.	40
Figure S11. MS/MS product ion mass spectrum from [M+H] ⁺ adduct of quercetin-rhamno-di-hexoside.	42
Table S1. Pairwise phenotypic Pearson correlations between the nine major cardenolides quantified from <i>Asclepias curassavica</i> leaves grown in a common environment (n=212).	43
Table S2. Principal component analysis loadings for the nine individual cardenolides on the two main principal components (Eigen values >1) for plant (85% variation explained) and monarch (72% variation explained) tissues.	45
Table S3. PERMANOVA results analyzing metabolic data based on Bray-Curtis dissimilarities.	46
Table S4. The relative inhibitory potential of seven isolated cardenolides on the sensitive porcine and typically-resistant monarch butterfly Na-K-ATPase (See also Figure 3).	47
Table S5. Poisson GLM model fits for predicting monarch oviposition on 212 <i>Asclepias curassavica</i> plants in a common greenhouse environment.	48
Table S6. Effects of two quercetin glycosides on monarch butterfly oviposition, tested with pure compounds in cages. >1 gram fresh leaf equivalent of each compound was added to each sponge.	49
Table S7. HRMS data of the cardenolides ions detected in samples.	50

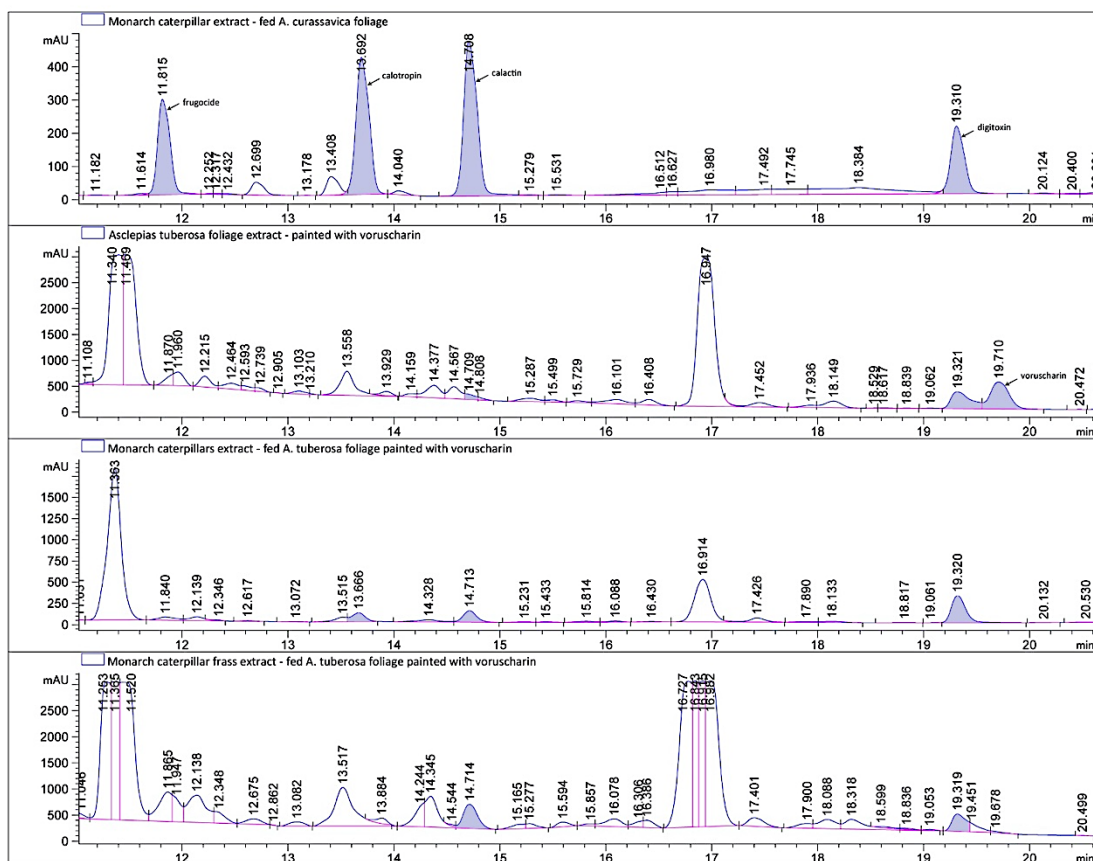


Fig. S1. Sample HPLC chromatograms.

(A) Monarch caterpillar feeding on *Asclepias curassavica*, (B) *A. tuberosa* foliage painted with voruscharin, (C) monarch caterpillars fed *A. tuberosa* painted with voruscharin, and (D) monarch frass from feeding on *A. tuberosa* painted with voruscharin. Digitoxin (RT 19.31-19.32) was added as the internal standard.

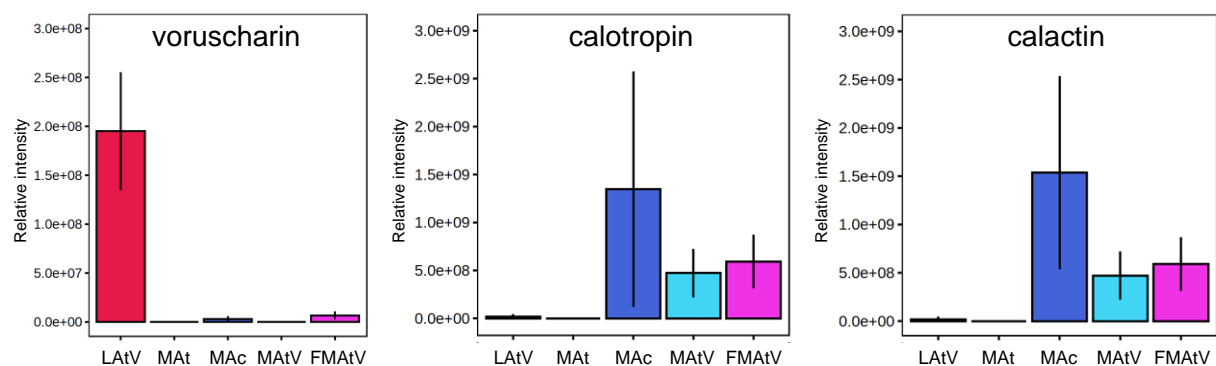


Fig. S2. Voruscharin painted on cardenolide-free milkweed leaves of *A. tuberosa* are converted to calactin and calotropin as revealed by LC-ESI- HRMS (n=4).

Ion mass of voruscharin, calactin and calotropin respectively detected at 590.2775 ($[M+H]^+$), 533.2745 ($[M+H]^+$), and 590.2741 ($[M+H]^+$) in positive ionization mode. Shown are means \pm SE relative concentrations (normalized mass spec ion abundance). LAtV: leaf of *A. tuberosa* painted with voruscharin; MAat: monarchs on *A. tuberosa*; MAc: monarchs on *A. curassavica*; MAatV: monarchs on *A. tuberosa* painted with voruscharin; FMAatV: frass from monarchs fed *A. tuberosa* painted with voruscharin.

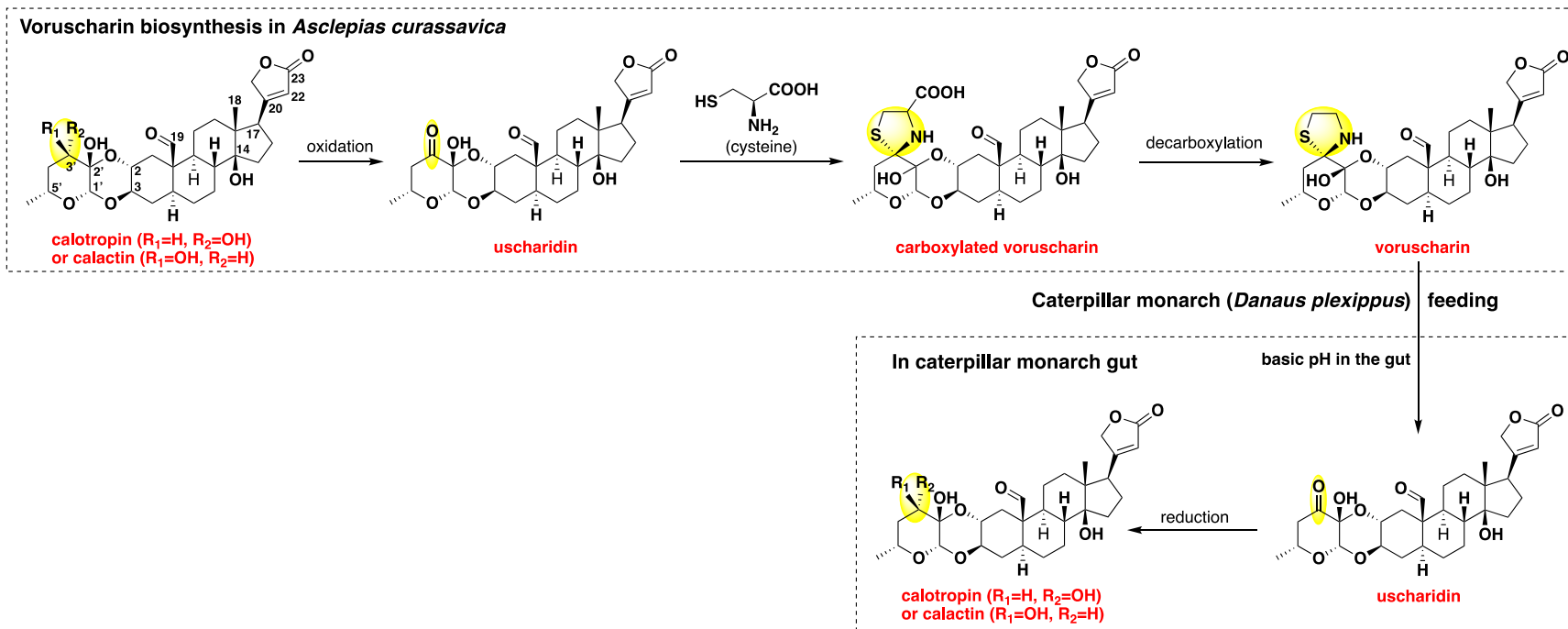


Fig. S3. Voruscharin putative biosynthesis in *Asclepias curassavica* and its degradation pathway in monarch gut.
The functional group in position C3' is highlighted in yellow to show the successive steps leading from calactin/calotropin to voruscharin.

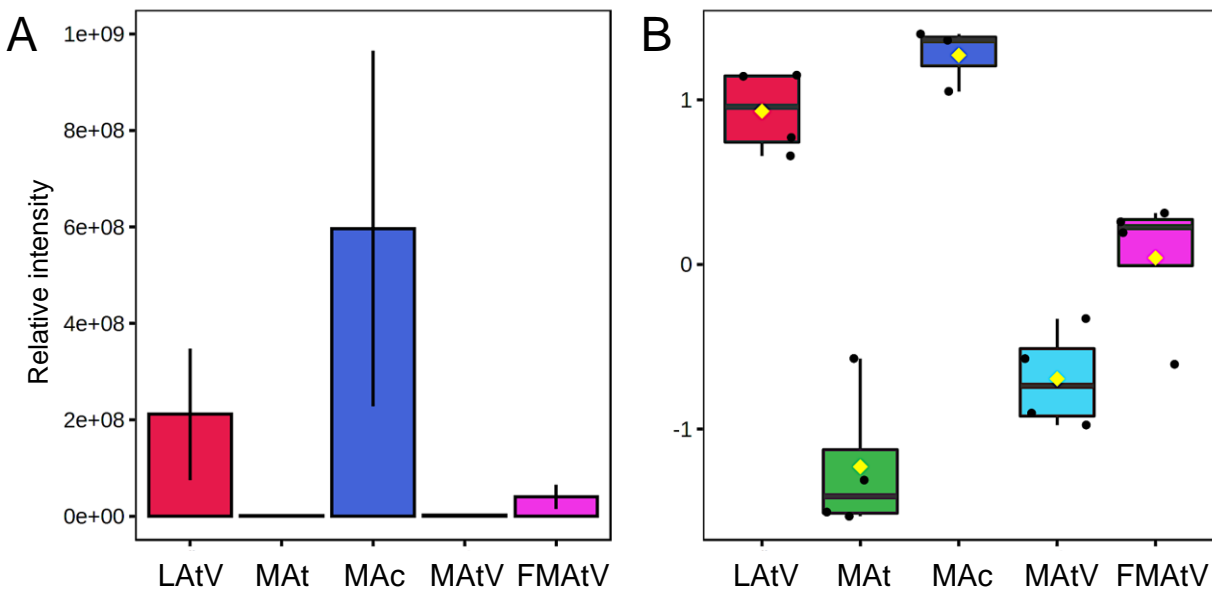


Fig. S4. Uscharidin relative concentrations in samples.

The bar plots show (A) the original values (mean +/- SD). The box and whisker plots (B) summarize the normalized values. The mean concentration of each group is indicated with a yellow diamond. Ion mass detected at 531.2588 ($[M+H]^+$) in positive ionization mode. LAtV: leaf of *A. tuberosa* painted with voruscharin; MAt: monarchs on *A. tuberosa*; MAc: monarchs on *A. curassavica*; MAtV: monarchs on *A. tuberosa* painted with voruscharin; FMAAtV: frass from monarchs fed *A. tuberosa* painted with voruscharin.

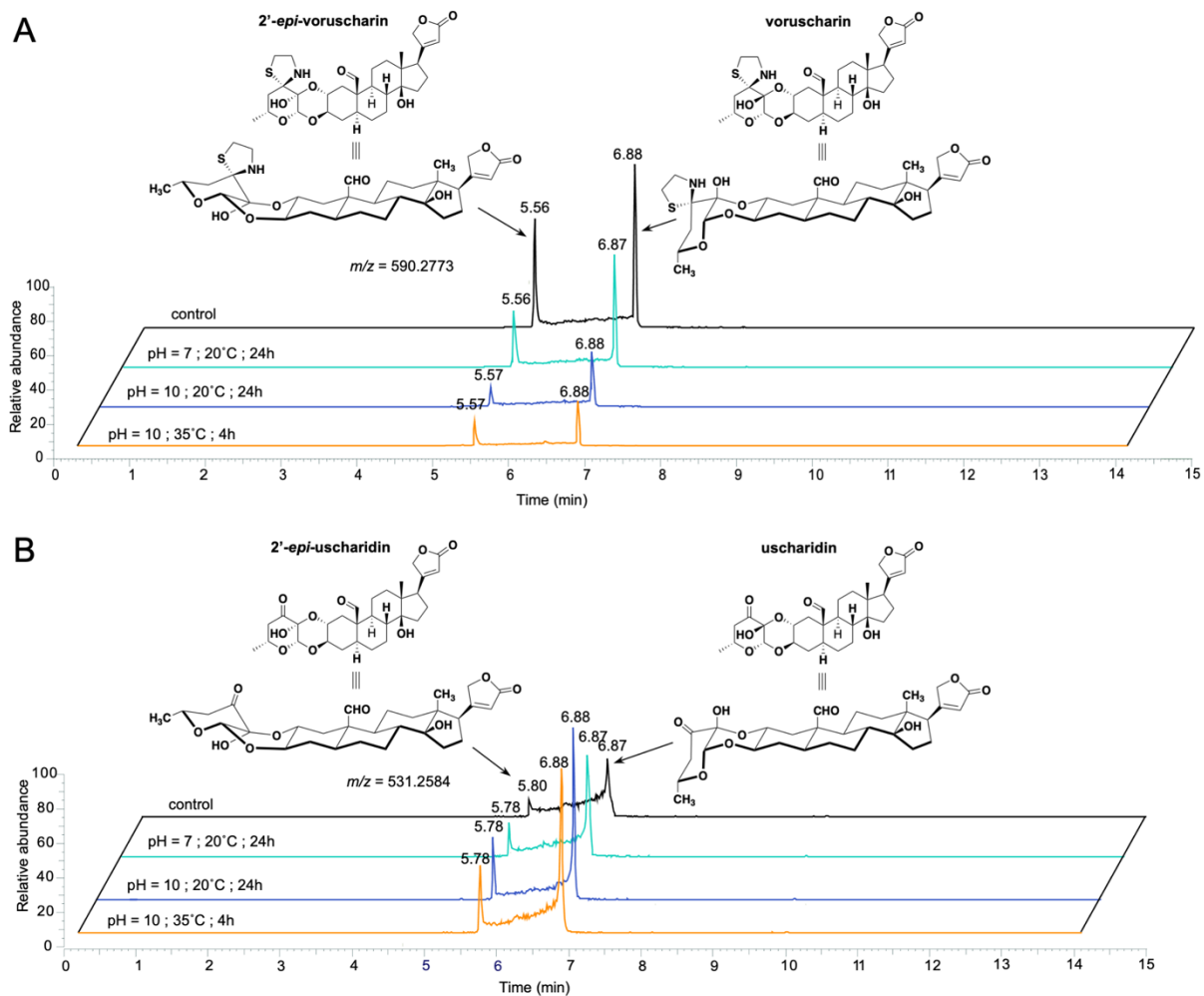


Fig. S5. Voruscharin stability assay at different pH values.

Chromatograms of voruscharin (A) and uscharidin (B), and corresponding epimers, after being stored at different temperatures and pH values. The control was stored at -20°C for 24h. The epimer's retention times was anticipated based on previous results of 2'-*epi*-uscharidin (1).

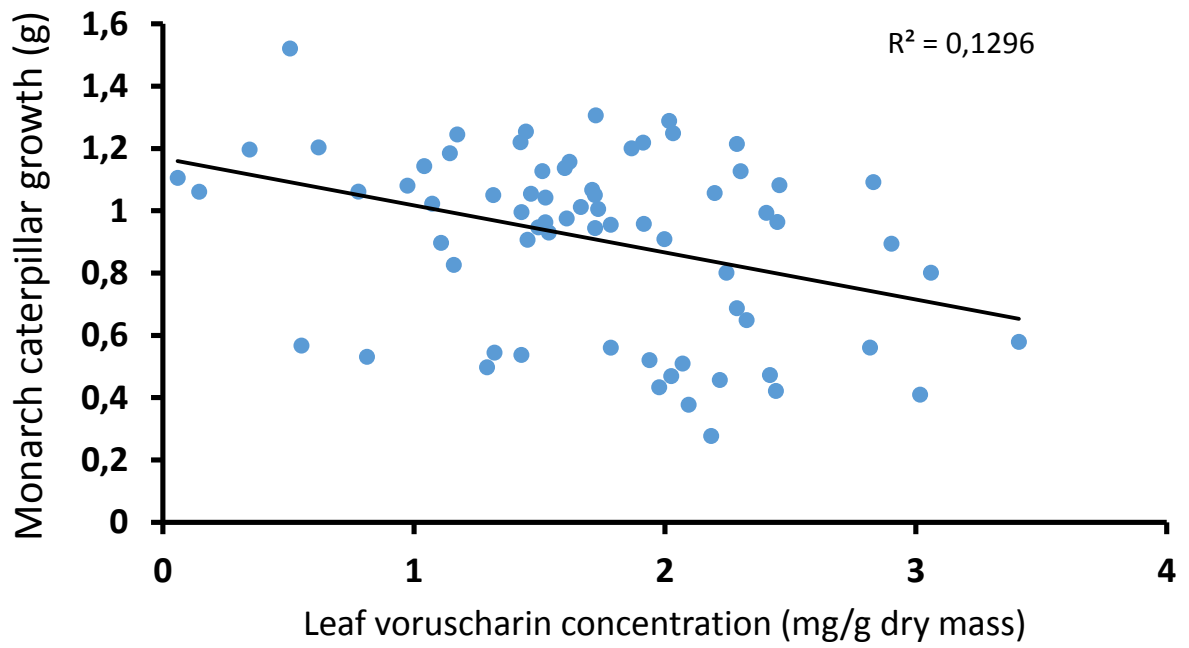
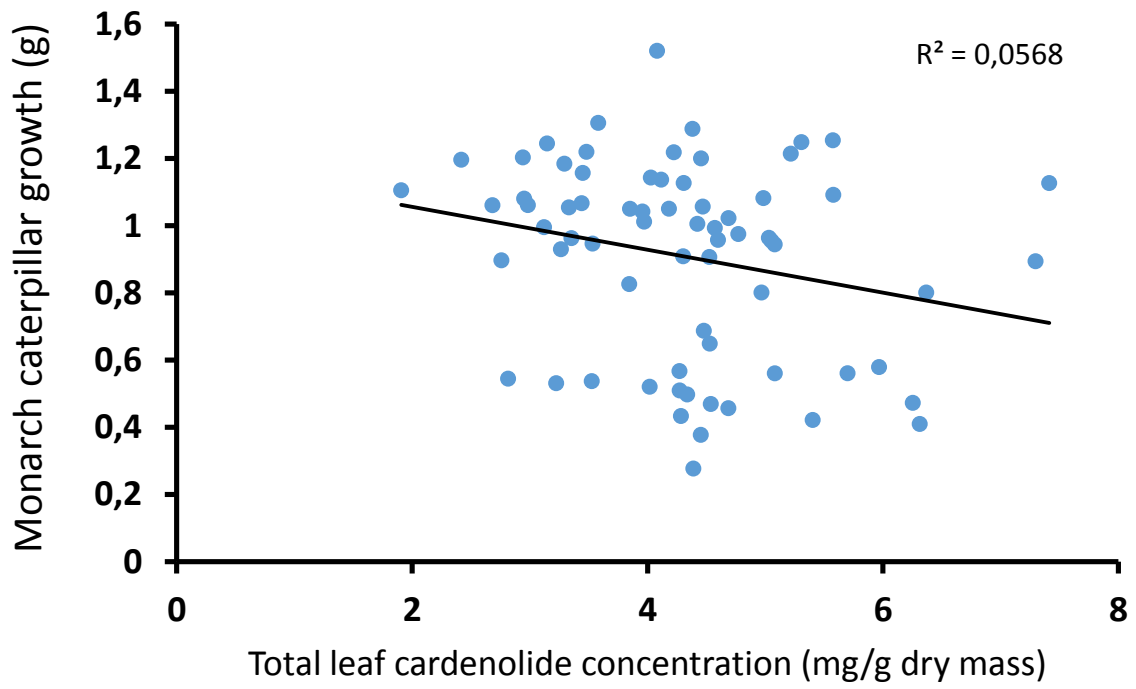


Fig. S6. Monarch caterpillar growth predicted by A) total leaf cardenolide and B) leaf voruscharin concentrations.

Note the weak relationships compared to sequestered cardenolides presented in Fig. 2 (and main text, which explained >60% of the variation in caterpillar growth).

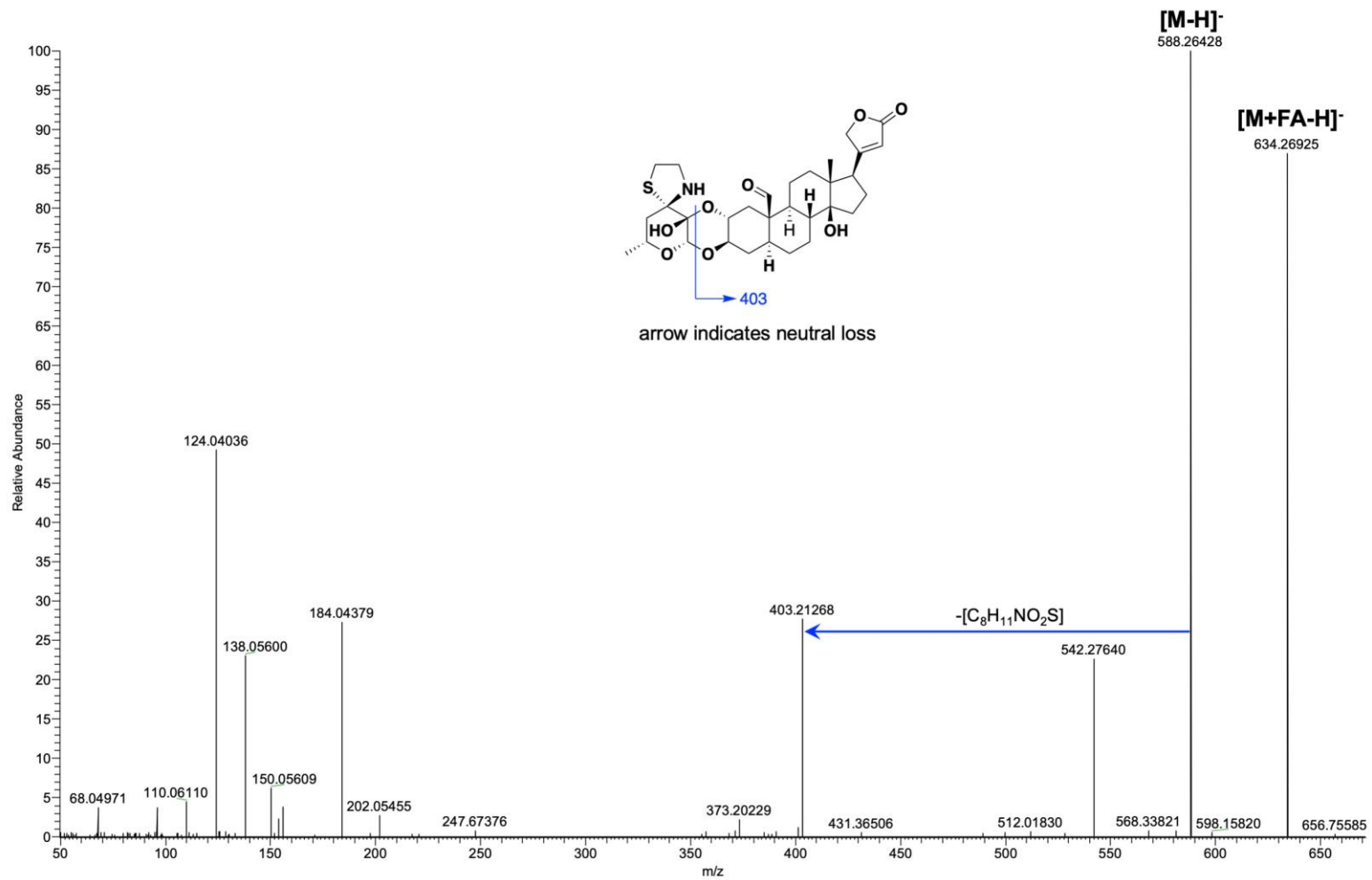


Fig. S7. MS/MS product ion mass spectrum from [M+FA-H]⁻ adduct of voruscharin.

The MS² spectrum of voruscharin was deposited to the GNPS database.

<https://gnps.ucsd.edu/ProteoSAFe/gnpslibraryspectrum.jsp?SpectrumID=CCMSLIB00005724352#%7B%7D>

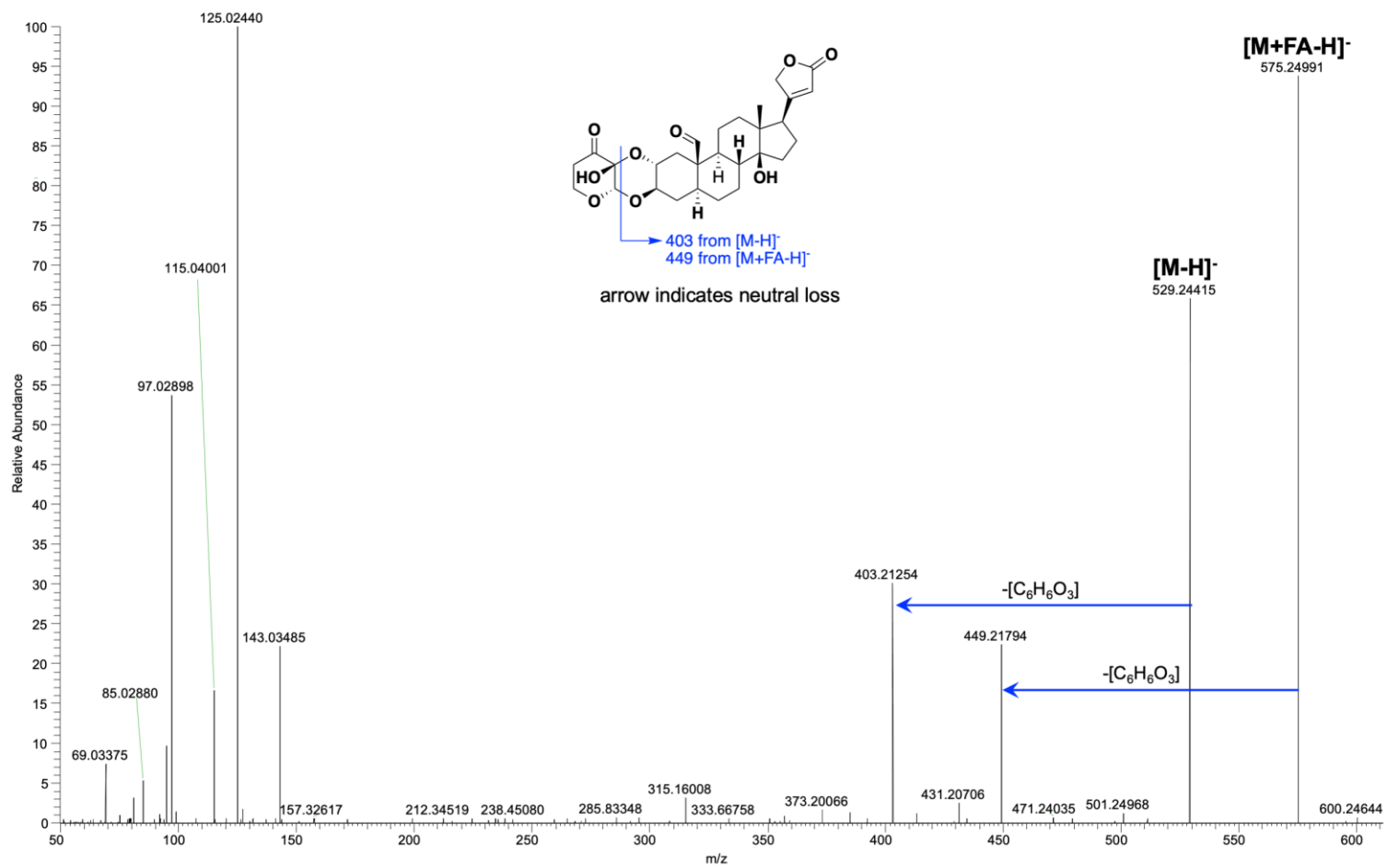


Figure S8. MS/MS product ion mass spectrum from [M+FA-H]⁻ adduct of uscharidin.

The MS² spectrum of uscharidin was deposited to the GNPS database.

<https://gnps.ucsd.edu/ProteoSAFe/gnpslibraryspectrum.jsp?SpectrumID=CCMSLIB00005724353#%7B%7D>

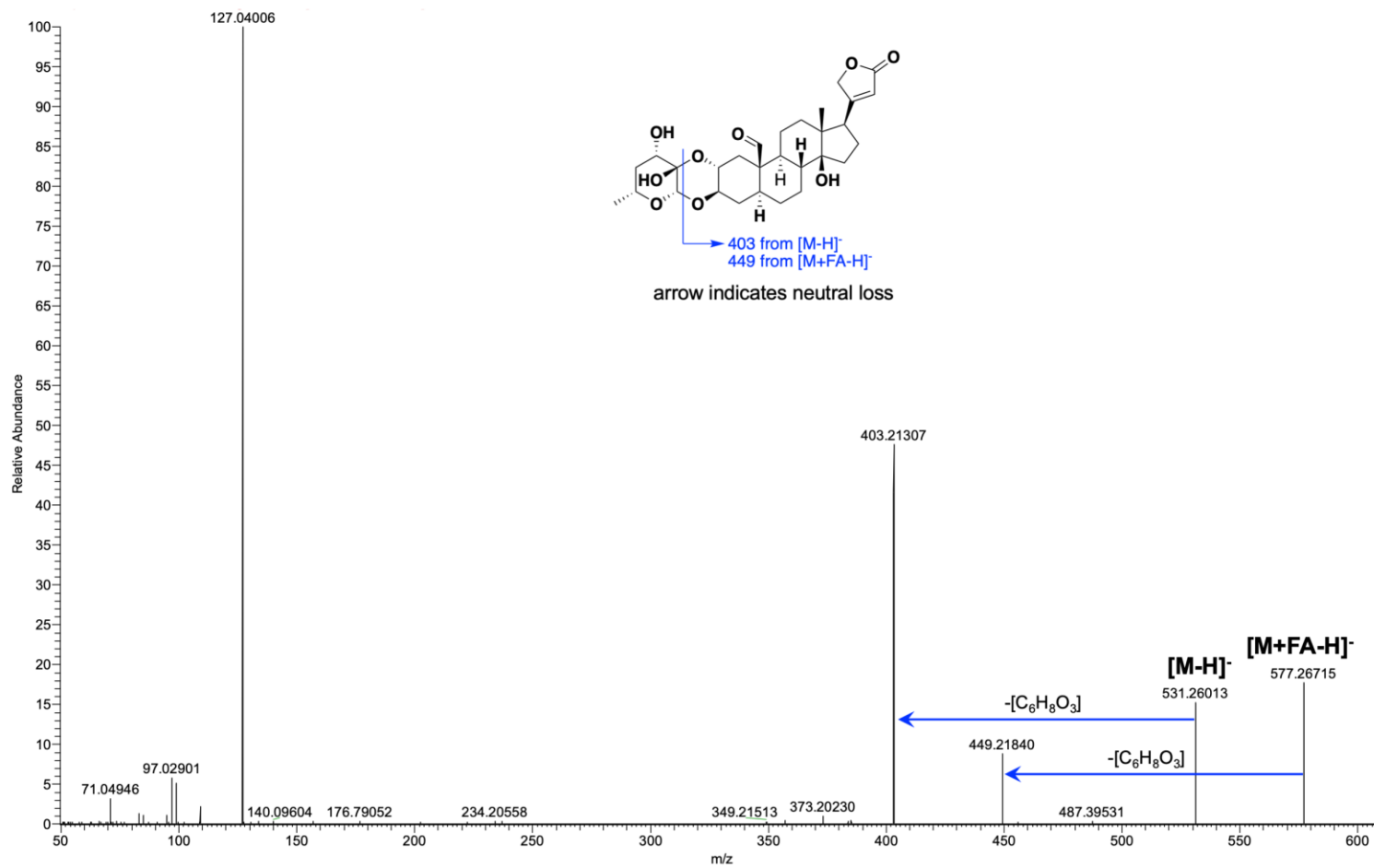


Figure S9. MS/MS product ion mass spectrum from [M+FA-H]⁻ adduct of calotropin.
The MS² spectrum of calactin/calotropin was deposited to the GNPS database.

<https://gnps.ucsd.edu/ProteoSAFe/gnpslibraryspectrum.jsp?SpectrumID=CCMSLIB00005724354#%7B%7D>

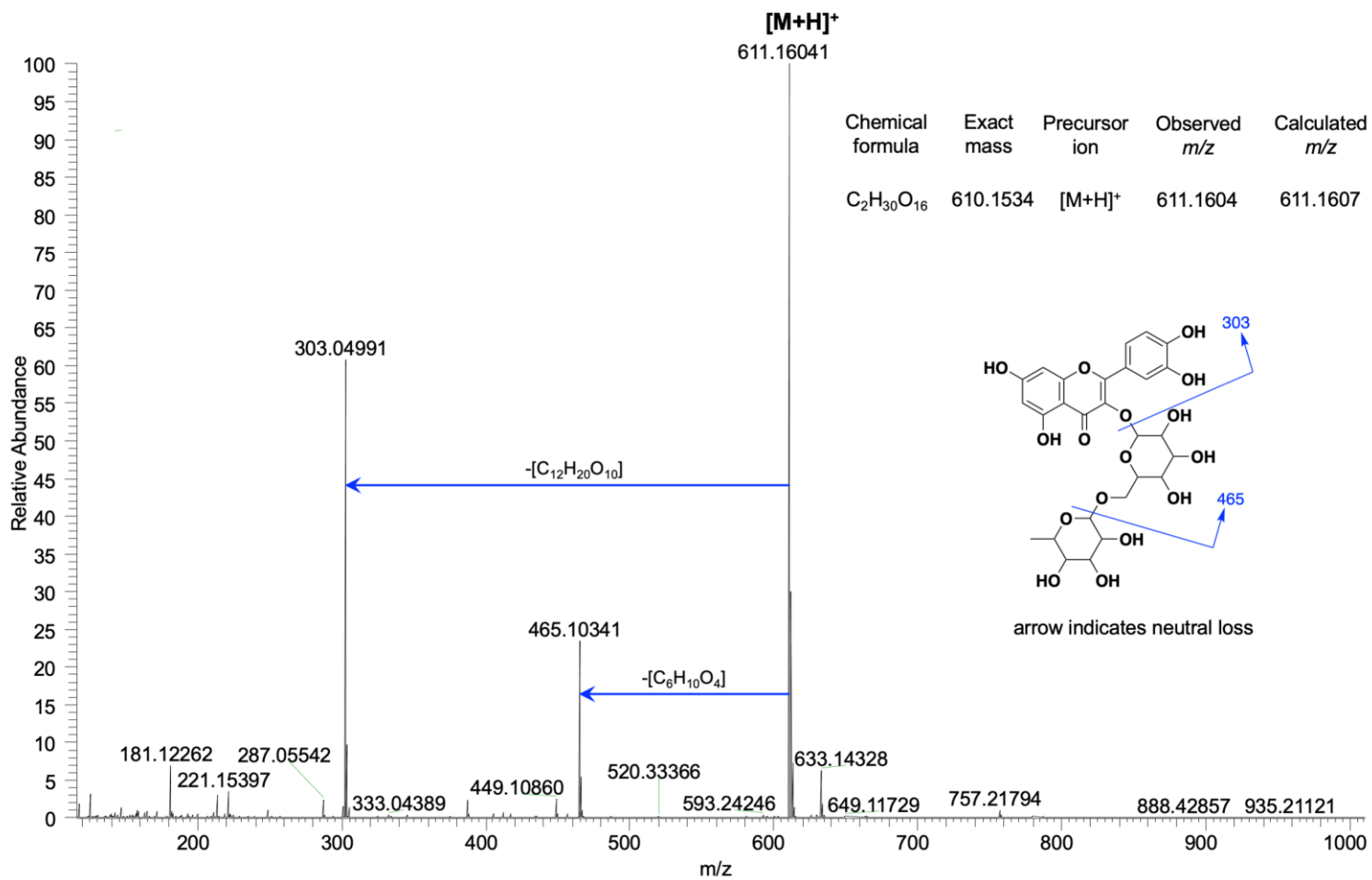


Figure S10. MS/MS product ion mass spectrum from [M+H]⁺ adduct of quercetin-rhamno-hexoside.

Based on previous phytochemical studies of characterized flavonols in *A. curassavica* (2) the structure is either quercetin 3-O- α -(2''-O- α -L-rhamnopyranosyl)- β -D-galactopyranoside or quercetin 3-O- α -(2''-O- α -L-rhamnopyranosyl)- β -D-glucopyranosyl (rutin).

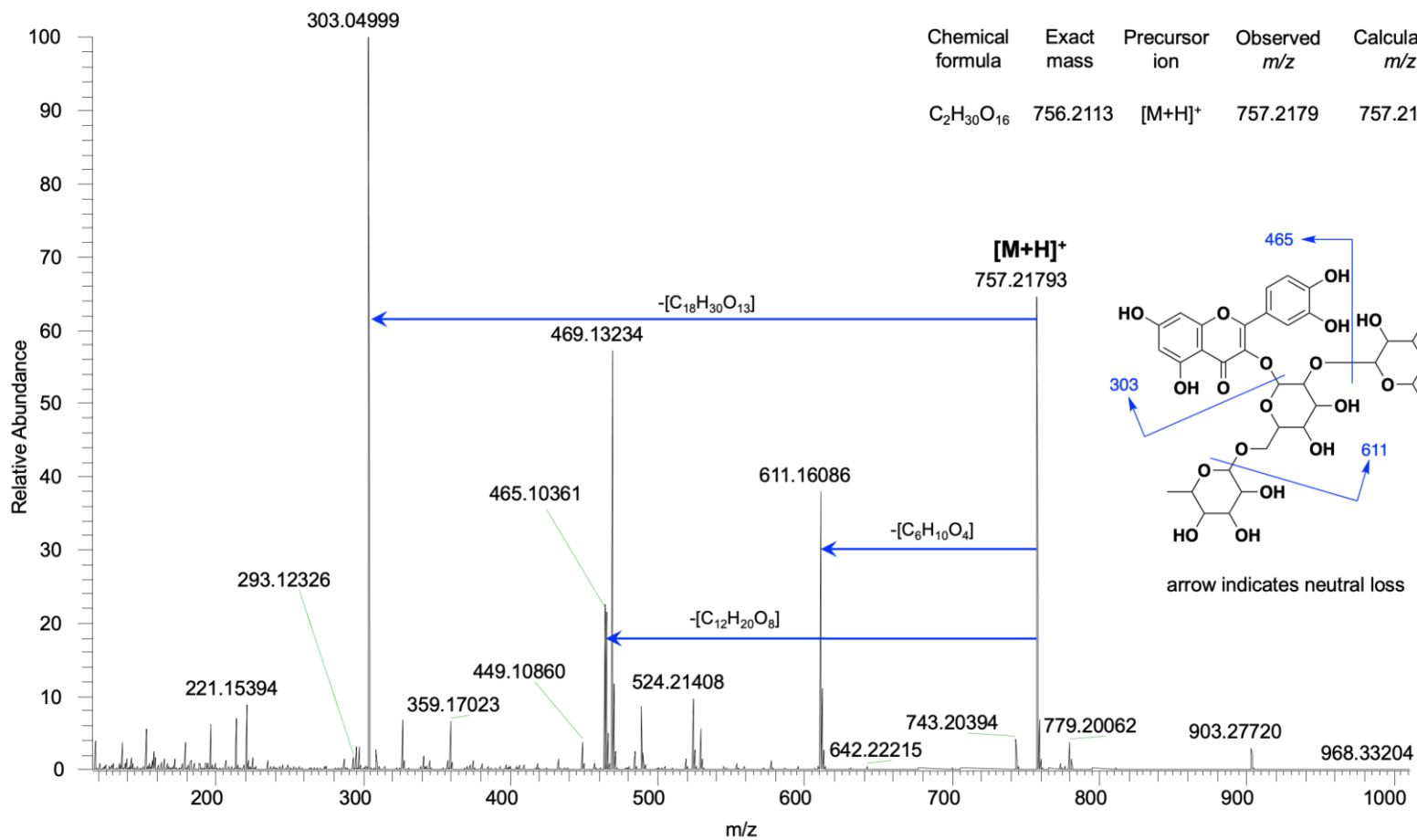


Figure S11. MS/MS product ion mass spectrum from [M+H]⁺ adduct of quercetin-rhamno-di-hexoside.

Based on previous phytochemical studies of characterized flavonols in *A. curassavica* (2) the structure is either quercetin 3-O-(2",6"-di- α -L-rhamnopyranosyl)- β -D-galactopyranoside or quercetin 3-O-(2",6"-O-di- α -L-rhamnopyranosyl)- β -D-glucopyranoside.

1 **Table S1. Pairwise phenotypic Pearson correlations between the nine major cardenolides**
 2 **quantified from *Asclepias curassavica* leaves grown in a common environment (n=212).**

3 Where compounds were not identified their retention time is given. Four non-significant
 4 correlations are highlighted in grey.

5
 6

		r	P
Frugoside	9.95	0.609	<.0001
12.54	9.95	0.666	<.0001
12.54	Frugoside	0.642	<.0001
14.66	9.95	0.757	<.0001
14.66	Frugoside	0.722	<.0001
14.66	12.54	0.905	<.0001
Calactin	9.95	0.727	<.0001
Calactin	Frugoside	0.747	<.0001
Calactin	12.54	0.820	<.0001
Calactin	14.66	0.950	<.0001
asclepin	9.95	0.405	<.0001
asclepin	Frugoside	0.795	<.0001
asclepin	12.54	0.426	<.0001
asclepin	14.66	0.521	<.0001
asclepin	Calactin	0.577	<.0001
18.18	9.95	0.693	<.0001
18.18	Frugoside	0.636	<.0001
18.18	12.54	0.913	<.0001
18.18	14.66	0.933	<.0001
18.18	Calactin	0.858	<.0001
18.18	asclepin	0.418	<.0001
Uscharin	9.95	0.145	0.0351

Uscharin	Frugoside	0.581	<.0001
Uscharin	12.54	0.238	0.0005
Uscharin	14.66	0.288	<.0001
Uscharin	Calactin	0.377	<.0001
Uscharin	asclepin	0.785	<.0001
Uscharin	18.18	0.228	0.0008
Voruscharin	9.95	-0.018	0.7917
Voruscharin	Frugoside	0.422	<.0001
Voruscharin	12.54	-0.035	0.6154
Voruscharin	14.66	0.063	0.3654
Voruscharin	Calactin	0.161	0.0191
Voruscharin	asclepin	0.569	<.0001
Voruscharin	18.18	-0.037	0.5885
Voruscharin	Uscharin	0.675	<.0001

8 **Table S2. Principal component analysis loadings for the nine individual cardenolides on**
 9 **the two main principal components (Eigen values >1) for plant (85% variation explained)**
 10 **and monarch (72% variation explained) tissues.**

11 Also shown is the average percentage of that each compound relative to the total cardenolide
 12 concentrations. Note that cardenolide compounds are not identical for the two tissues and the
 13 PC analyses are completely independent. Compounds are ordered by retention time (RT).

14

	Cardenolide	% of the total	PC axis 1	PC axis 2
Plant tissue ¹ (n=212)				
	RT9.95	6.3	0.767	-0.312
	Frugoside	6.0	0.876	0.249
	RT12.54	4.0	0.865	-0.346
	RT14.66	11.4	0.939	-0.278
	Calactin	5.1	0.934	-0.153
	Asclepin	12.2	0.739	0.555
	RT18.18	4.1	0.877	-0.365
	Uscharin	10.9	0.533	0.741
	Voruscharin	39.9	0.283	0.843
Insect tissue ² (n=70)				
	RT5.6	3.3	0.651	-0.476
	RT8	6.5	0.792	-0.316
	RT8.3	1.5	0.498	0.709
	RT9.5	5.9	0.643	0.282
	Frugoside	22.5	0.869	0.119
	RT12.8	2.7	0.901	-0.136
	RT13.5	2.7	0.805	0.077
	Calotropin	22.8	0.878	0.185
	Calactin	32.1	0.866	-0.207

15

16 ¹ PC axes are orthogonal and both are highly significant in explaining variation in total plant
 17 cardenolides (PC1 R²=0.50, PC2 R²=0.43).

18

19 ² PC axes are orthogonal and only PC1 was significant in explaining variation in total cardenolides
 20 sequestered by monarchs (PC1 R²=0.97).

21

22

23 **Table S3. PERMANOVA results analyzing metabolic data based on Bray-Curtis**
 24 **dissimilarities.**
 25

Source of variation	DF	SumSq	MeanSqs	F. model	R ²	P
All chemical extracts	4	0.067220	0.0168050	60.8942	0.6477	0.001
Residuals	15	0.036563	0.0024376		0.3523	
Total	19	0.103783			1.0000	
<i>Pairwise</i>						
LAtV × MAt	1	0.039476	0.039476	3.429	0.36367	0.037
LAtV × MAc	1	0.045634	0.045634	2.1744	0.266	0.123
LAtV × MAtV	1	0.026582	0.026582	1.7521	0.22601	0.143
LAtV × FMAtV	1	0.020933	0.020932	1.3962	0.18877	0.181
MAt × MAc	1	0.024287	0.024287	2.2136	0.26951	0.121
MAt × MAtV	1	0.026924	0.0269240	6.3835	0.51548	0.002
MAt × FMAtV	1	0.033727	0.033727	4.3275	0.41902	0.036
MAc × MAtV	1	0.028296	0.0282957	3.4997	0.3684	0.024
MAc × FMAtV	1	0.046877	0.046877	3.2347	0.35028	0.033
MAtV × FMAtV	1	0.021856	0.0218561	2.2519	0.27289	0.038

26

27 LAtV: Leaf of *A. tuberosa* painted with voruscharin; MAt: Monarchs on *A. tuberosa*;

28 MAc: Monarchs on *A. curassavica*; MAtV: Monarchs on *A. tuberosa* painted with voruscharin;

29 FMAtV: Frass from monarchs fed *A. tuberosa* painted with voruscharin.

30 DF - degrees of freedom; SumSq - sum of squares; MeanSqr - mean squares.

31 P-values based on 999 permutations (lowest P-value possible 0.001).

32 **Table S4. The relative inhibitory potential of seven isolated cardenolides on the sensitive**
33 **porcine and typically-resistant monarch butterfly Na-K-ATPase (See also Figure 3).**

34 IC_{50} is the concentration (μ M) at which the enzyme is inhibited by 50%. Sequestered+ indicates
35 that these compounds are sequestered intact from consumed leaves as well as converted
36 products from consumed voruscharin and uscharin.

37

38

	Porcine ATPase (IC_{50})	Monarch ATPase (IC_{50})	IC_{50} ratio	Total n
Ouabain (standard)	0.81	122.09	151	11
Digitoxin (standard)	0.49	16.25	33	12
Frugoside (sequestered)	0.37	27.80	76	8
Calotropin (sequestered+)	0.27	10.90	40	6
Calactin (sequestered+)	0.24	3.21	13	6
Uscharin (unsequestered)	0.78	1.00	1	12
Voruscharin (unsequestered)	0.46	2.02	4	26

39

40

41

42 **Table S5. Poisson GLM model fits for predicting monarch oviposition on 212 *Asclepias***
 43 ***curassavica* plants in a common greenhouse environment.**

44 Breaking down the predictors by cardenolide principal components, the four of nine significant
 45 individual cardenolides, and two quercetin glycosides (there was no indication of a quadratic fit
 46 for the quercetin glycosides). Voruscharin concentration dominates PC2 and was not a
 47 significant predictor in individual analyses.

48
 49

Plant compound	Factor	L-R χ^2	p
PC1	PC1	4.687	0.030
	PC1 squared	5.317	0.021
	Plant height	14.628	<0.001
PC2	PC2	0.2249	0.617
	PC2 squared	0.135	0.713
	Plant height	13.746	<0.001
Frugoside	Frugoside	6.156	0.013
	Frugoside squared	6.161	0.013
	Plant height	12.677	<0.001
Calactin	Calactin	6.228	0.013
	Calactin squared	5.282	0.022
	Plant height	16.529	<0.001
RT14.66	RT14.66	7.386	0.007
	RT14.66 squared	6.978	0.008
	Plant height	14.907	<0.001
RT18.18	RT18.18	7.388	<0.001
	RT18.18 squared	8.053	0.004
	Plant height	14.657	<0.001
Quercetin glycosides	quercetin-rhamno-di-hexoside ¹	0.115	0.731
	quercetin-rhamno-hexoside ²	0.002	0.960
	Plant height	14.285	<0.001

50

51 ¹ Molecular mass 756 g/mol

52 ² Molecular mass 610 g/mol

53 **Table S6. Effects of two quercetin glycosides on monarch butterfly oviposition, tested**
54 **with pure compounds in cages. >1 gram fresh leaf equivalent of each compound was**
55 **added to each sponge.**

56 A mixed-model ANOVA was used (random effect was blocking cage): overall effect of treatment
57 $F_{2,27.98}=9.901$, $p<0.001$.

58

59

Compound	Eggs laid (LS mean)	Standard error	Tukey comparison
Control	39.6	12.2	A
quercetin-rhamno-di-hexoside ¹	44.8	13.7	A
quercetin-rhamno-hexoside ²	84.9	14.2	B

60

61 ¹ Molecular mass 756 g/mol

62 ² Molecular mass 610 g/mol

63 **Table S7. HRMS data of the cardenolides ions detected in samples.**

64 To simplify the table, only MS data from one replicate is listed for each precursor ion.

65

Cardenolide	Formula	Precursor ion	Observed <i>m/z</i>	Calculated <i>m/z</i>	$\Delta m/z$ (ppm)	Sample (replicate number)
Voruscharin	C ₃₁ H ₄₃ NO ₈ S	[M+H] ⁺	590.2781	590.2775	-1.0	<i>A. tuberosa</i> vor. Treated foliage (1)
				590.2782	0.1	Frass from cats (1)
				590.2782	0.1	Frass from cats (1)
		[M+Na] ⁺	612.2601	612.2592	-1.4	<i>A. tuberosa</i> vor. Treated foliage (1)
				612.2605	0.6	Frass from cats (1)
				612.2605	0.6	Frass from cats (1)
		[M-H] ⁻	588.2636	588.2634	-0.3	<i>A. tuberosa</i> vor. Treated foliage (1)
				588.2648	2.0	Frass from cats (1)
				588.2648	2.0	Frass from cats (1)
[M+FA-H] ⁻	634.2691	634.2689	-0.3	<i>A. tuberosa</i> vor. Treated foliage (1)		
		634.2689	-0.3	Frass from cats (1)		
		634.2689	-0.3	Frass from cats (1)		
Uscharidin	C ₂₉ H ₃₈ O ₉	[M+H] ⁺	531.2588	531.2585	-0.5	<i>A. tuberosa</i> vor. Treated foliage (1)
				531.2588	0.0	Frass from cats (1)
				531.2592	0.7	<i>A. curassavica</i> feds cats (1)
				531.2592	0.7	<i>A. curassavica</i> feds cats (1)
				531.2592	0.7	<i>A. curassavica</i> feds cats (1)
		[M+Na] ⁺	553.2408	553.2403	-0.9	<i>A. tuberosa</i> vor. Treated foliage (1)
				553.2402	-1.0	Frass from cats (1)
				553.2416	1.4	<i>A. curassavica</i> feds cats (1)
		[M-H] ⁻	529.2443	529.2440	-0.5	<i>A. tuberosa</i> vor. Treated foliage (1)
				529.2443	0.0	Frass from cats (1)
				529.2443	0.0	<i>A. curassavica</i> feds cats (1)
		[M+FA-H] ⁻	575.2498	575.2498	0.0	<i>A. tuberosa</i> vor. Treated foliage (1)
				575.2501	0.5	Frass from cats (1)
				575.2500	0.3	<i>A. curassavica</i> feds cats (1)
		Calotropin	C ₂₉ H ₄₀ O ₉	[M+H] ⁺	533.2744	533.2737
533.2745	0.1					Frass from cats (1)
533.2740	-0.7					<i>A. curassavica</i> feds cats (1)
[M+Na] ⁺	555.2564			555.2549	-2.7	<i>A. tuberosa</i> fed cats w/ voruscharin (1)
				555.2546	-3.2	Frass from cats (1)
				555.2553	-1.9	<i>A. curassavica</i> feds cats (1)
[M-H] ⁻	531.2599			531.2590	-1.6	<i>A. tuberosa</i> fed cats w/ voruscharin (1)
				531.2612	2.4	Frass from cats (1)
				531.2597	-0.3	<i>A. curassavica</i> feds cats (1)
[M+FA-H] ⁻	577.2654			577.2655	0.1	<i>A. tuberosa</i> fed cats w/ voruscharin (1)

				577.2659	0.8	voruscharin (1)
				577.2665	1.9	Frass from cats (1)
						<i>A. curassavica</i> feds cats (1)
Calactin	C ₂₉ H ₄₀ O ₉	[M+H] ⁺	533.2744	533.2733	-2.0	<i>A. tuberosa</i> fed cats w/ voruscharin (1)
				533.2741	-0.5	Frass from cats (1)
				533.2742	-0.3	<i>A. curassavica</i> feds cats (1)
		[M+Na] ⁺	555.2564	555.2552	-2.1	<i>A. tuberosa</i> fed cats w/ voruscharin (1)
				not detected	-	Frass from cats (1)
				555.2554	-1.8	<i>A. curassavica</i> feds cats (1)
		[M-H] ⁻	531.2599	531.2596	-0.5	<i>A. tuberosa</i> fed cats w/ voruscharin (1)
				531.2593	-1.1	Frass from cats (1)
				531.2596	-0.5	<i>A. curassavica</i> feds cats (1)
		[M+FA-H] ⁻	577.2654	577.2654	0.0	<i>A. tuberosa</i> fed cats w/ voruscharin (1)
				577.2659	0.8	Frass from cats (1)
				577.2664	1.7	<i>A. curassavica</i> feds cats (1)

66

67

68 **References**

69

70 1. Parhira S, Zhu G-Y, Jiang R-W, Liu L, Bai L-P, & Jiang Z-H (2014) 2'-*Epi*-uscharin from the
71 latex of *Calotropis gigantea* with HIF-1 inhibitory activity. *Sci. Rep.* 4:4748.

72

73 2. Haribal M & Renwick JA (1996) Oviposition stimulants for the monarch butterfly: flavonol
74 glycosides from *Asclepias curassavica*. *Phytochemistry* 41:139-144.

75